

Massive Diboson Measurements from ATLAS and CMS

Prachi Arvind Atmasiddha

On behalf of the ATLAS and CMS collaborations, CERN

30th August 2023

Multi-Boson Interactions Conference 2023, San Diego, USA

Contents

- Latest massive di-boson measurements from ATLAS and CMS include inclusive and differential cross-sections, EFT interpretations, polarization measurements and CP studies.
- Latest ATLAS di-boson measurements (total six analyses):
 - The channels include $ZZjj$, (Same sign) $W^\pm W^\pm jj$, (Opposite Sign) $W^+ W^-$ and with associated jets, (Opposite Sign) $W^+ W^- jj$, $W^\pm Z$.
- Latest CMS diboson measurements (total five analyses):
 - $W^\pm Z$, $WVjj$ Semi-leptonic, $ZZ + jets$, (Opposite Sign) $W^+ W^- jj$, $\gamma\gamma \rightarrow WW$ and $\gamma\gamma \rightarrow ZZ$.

$4\ell + jj$ Measurement Introduction

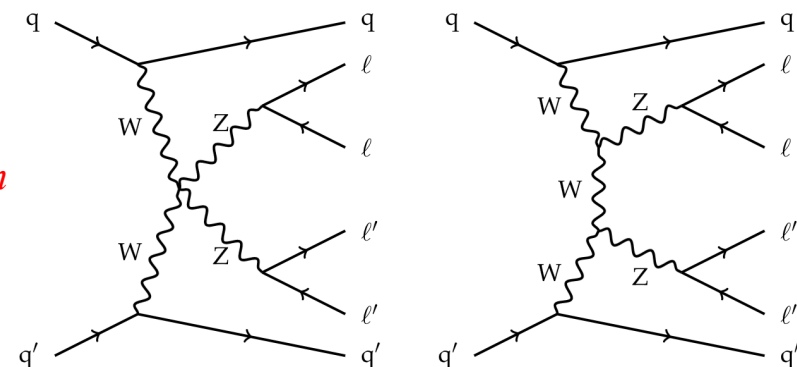
- $ZZjj$ observation with 139 fb^{-1} : 5.7 sigma (5.9 sigma) observed (expected) in Feb 2023. [Nature Physics 19, 237–253 \(2023\)](#)
- The latest analysis with an integrated luminosity of 140 fb^{-1} contains:
 - Differential cross-section measurements for the production of four charged leptons in association with two jets
 - limits on the anomalous weak boson self interactions..

Event Selection:

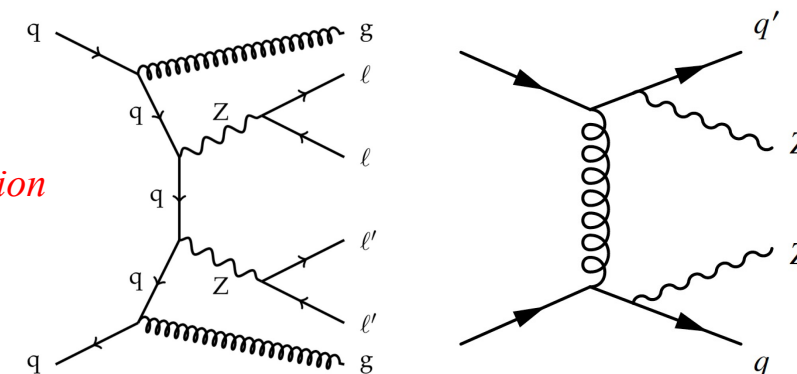
- $m_{4\ell} > 130 \text{ GeV}$
- At least two jets: Dijet system is defined as two leading jets in the event with $\eta_{j_1} \times \eta_{j_2} < 0$, $\Delta y_{jj} > 2.0$ and $m_{jj} > 300 \text{ GeV}$.
- VBS-enhanced and VBS-suppressed regions:
 - $\zeta < 0.4$ (VBS enhanced) and $\zeta > 0.4$ (VBS suppressed)

$$\zeta = \frac{(y_{4\ell} - 0.5(y_{j_1} + y_{j_2}))}{\Delta y_{jj}}$$

EW Production



Strong Production



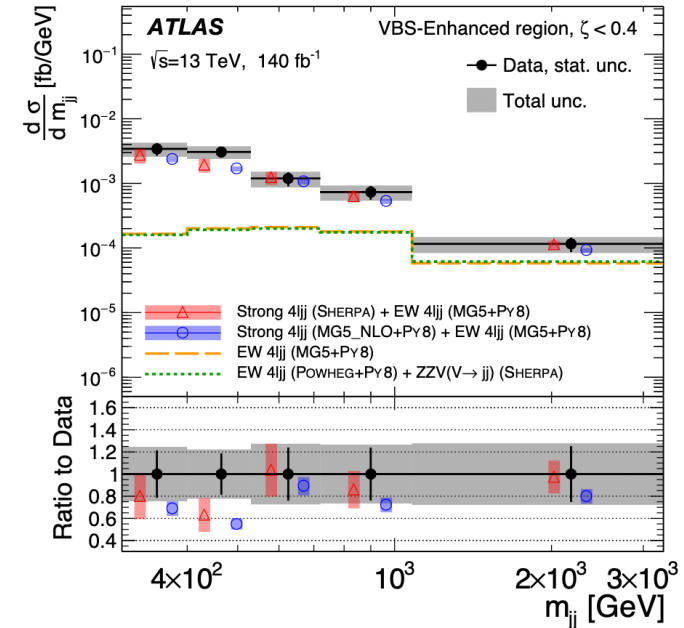
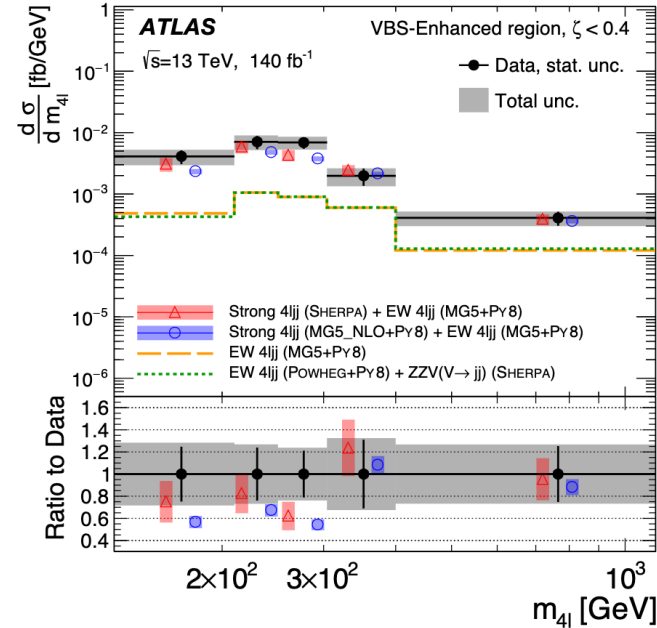
Backgrounds:

- **Prompt Background (15% of signal yield):** Processes with leptons that do not originate from the decay of a Z boson ($t\bar{t}Z$, WWZ , WZZ)
- **Non-prompt Background (2.4% of signal yield):** One or more non-prompt leptons ($WZjj$, $t\bar{t}$). Estimated using data-driven method.

$4\ell + jj$ Differential Cross-section

- Differential cross-section measurement as a function of observables:
 - Sensitive to the VBS process
 - those sensitive to the Z boson polarization and
 - those sensitive to the QCD interactions (higher order real emission of quarks and gluons).
- The distributions Unfolded using the iterative Bayesian unfolding procedure.
- Unfolding is performed in both VBS-enhanced and VBS-suppressed regions.

Source	Uncertainty (%)
Luminosity	0.8 – 1.3
Leptons	0.8 – 1.6
Jets	2.7 – 18
Pile-up	0.0 – 2.5
Backgrounds	0.9 – 9.0
Theory modelling	0.6 – 8.8
Unfolding method	0.9 – 12
Total systematic	5 – 22



The differential cross sections for inclusive $4\ell jj$ production in the VBS-enhanced region as a function of $m_{4\ell}$ and m_{jj} .

Results:

- EW contribution: 20% in VBS enhanced (50% in high m_{jj} and 5% in low m_{jj} region.)
- No significant difference observed between two different generators for EW $ZZjj$ distributions.

$4\ell + jj$ EFT Interpretations

- SM extended with new interactions included in the dim-8 operators of EFT formalism.

$$\mathcal{L} = \mathcal{L}_{\text{SM}} + \sum_i \frac{f_{\text{T},i}}{\Lambda^4} \mathcal{O}_{\text{T},i}$$

- Squared scattering amplitude for EFT prediction:

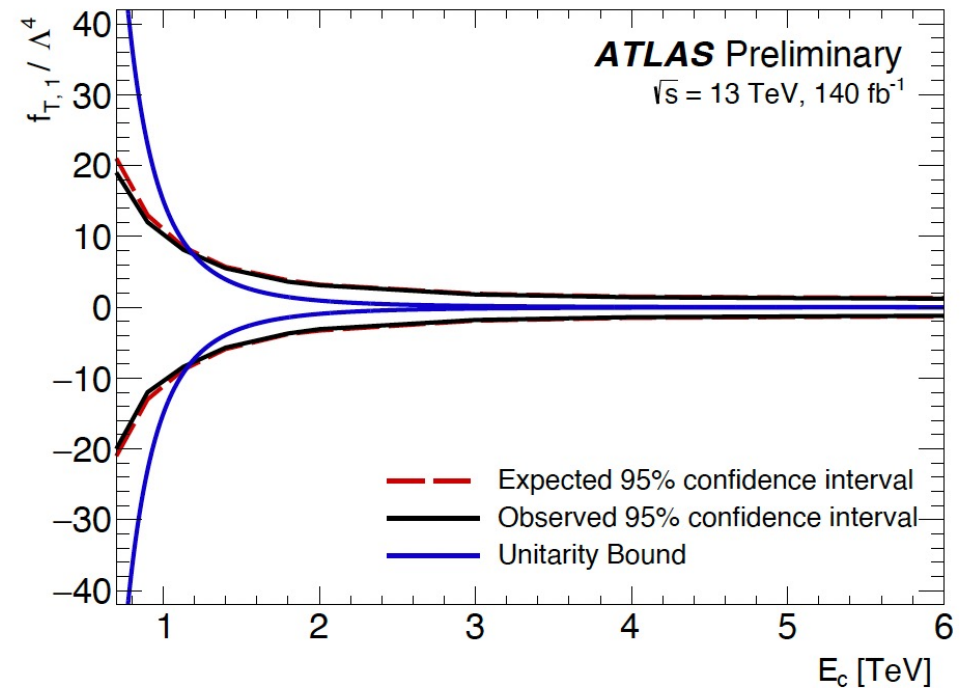
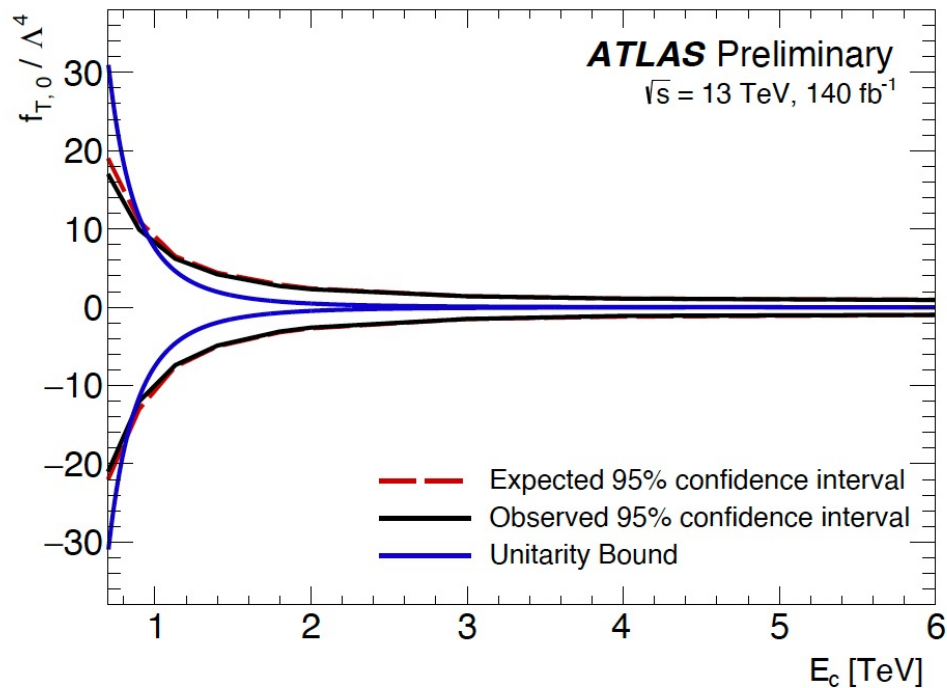
$$|\mathcal{M}|^2 = |\mathcal{M}_{\text{SM}}|^2 + 2 \text{Re}(\mathcal{M}_{\text{SM}}^* \mathcal{M}_{\text{d8}}) + |\mathcal{M}_{\text{d8}}|^2$$

- aQGC self interactions appear in lowest order as Dim-8 operators.
- Assumption is that contribution from dim-6 operators is 0 i.e. already constrained from diboson and VBF production (for completeness limits on dim-6 operators are also set.)
- The 95% confidence intervals and upper limits on the dimension-eight Wilson coefficients are calculated using a two-dimensional fit to the $4\ell jj$ differential cross-section as a function of $m_{4\ell}$ and m_{jj} .

Wilson coefficient	$\mathcal{M}_{\text{d8}} ^2$ Included	95% confidence interval [TeV ⁻⁴]	
		Expected	Observed
$f_{\text{T},0}/\Lambda^4$	yes	[-0.98, 0.93]	[-1.00, 0.97]
	no	[-23, 17]	[-19, 19]
$f_{\text{T},1}/\Lambda^4$	yes	[-1.2, 1.2]	[-1.3, 1.3]
	no	[-160, 120]	[-140, 140]
$f_{\text{T},2}/\Lambda^4$	yes	[-2.5, 2.4]	[-2.6, 2.5]
	no	[-74, 56]	[-63, 62]
$f_{\text{T},5}/\Lambda^4$	yes	[-2.5, 2.4]	[-2.6, 2.5]
	no	[-79, 60]	[-68, 67]
$f_{\text{T},6}/\Lambda^4$	yes	[-3.9, 3.9]	[-4.1, 4.1]
	no	[-64, 48]	[-55, 54]
$f_{\text{T},7}/\Lambda^4$	yes	[-8.5, 8.1]	[-8.8, 8.4]
	no	[-260, 200]	[-220, 220]
$f_{\text{T},8}/\Lambda^4$	yes	[-2.1, 2.1]	[-2.2, 2.2]
	no	[-4.6, 3.1]×10 ⁴	[-3.9, 3.8]×10 ⁴
$f_{\text{T},9}/\Lambda^4$	yes	[-4.5, 4.5]	[-4.7, 4.7]
	no	[-7.5, 5.5]×10 ⁴	[-6.4, 6.3]×10 ⁴

$4\ell + jj$ EFT Interpretations

- The inter- and pure dim-eight- contributions have $m_{4\ell} < E_c$.

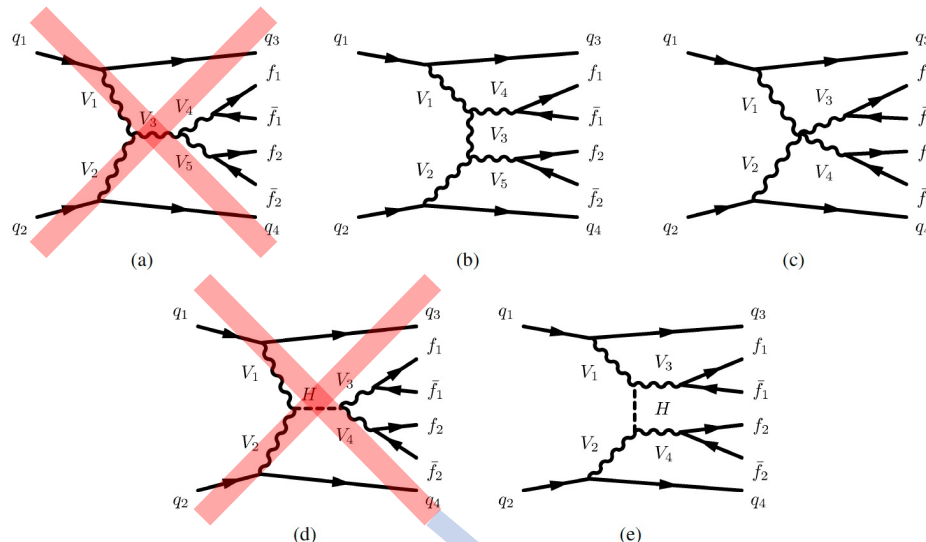


Exp and Obs 95% confidence interval for the Wilson coefficients as a function of a cut-off scale, E_c .

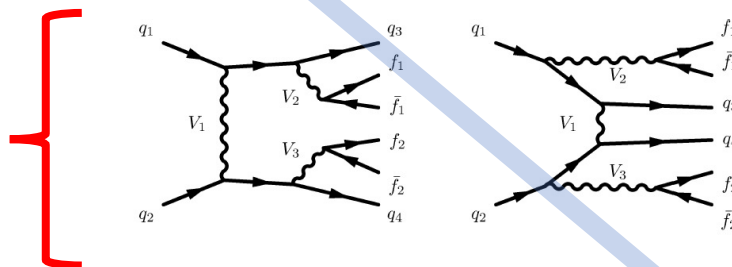
2

(Same sign) $W^\pm W^\pm jj$ Cross-section Measurement

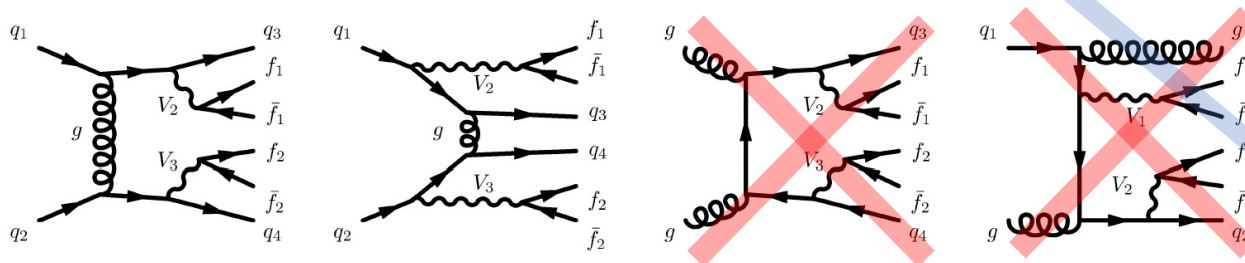
Electroweak
VBS VVjj



Electroweak non-VBS VVjj



Strong VVjj



X Forbidden in the SM and/or for $W^\pm W^\pm jj$

- Largest ratio of Electroweak to Strong productions cross-section compared to other VBS diboson processes (~ 5 for the fiducial region of this analysis).
- Observed before with 36.1 fb^{-1} : obs significance of 6.5σ ([PRL 123 \(2019\) 161801](#)).
- Measurements performed using integrated luminosity of 139 fb^{-1} :
 - EW and Inclusive (EW+Int+QCD) accuracy Inclusive and Differential Cross-sections in the fiducial phase space.
 - Limits on anomalous quartic gauge couplings
 - Limits on doubly charged Higgs production

(Same sign) $W^\pm W^\pm jj$ Cross-section Measurement

Event Selection:

- Expected purity of the EW, QCD and interference is 52%, 5.4% and 1.7%.
- Exactly two signal leptons
 - $m_{\ell\ell'} \geq 20$ GeV
 - 3rd lepton veto
- $E_T^{miss} \geq 30$ GeV
- At least two jets, b-jet veto applied
 - $m_{jj} \geq 500$ GeV: suppresses triboson production with resonant decay to two jets
 - $|\Delta y_{jj}| > 2$

Backgrounds:

- WZ/γ^* (22% of the signal event yield): One lepton escaping the third lepton veto requirement.
- Non-Prompt Lepton Background (12% of the signal event yield): $W + jets$, semi-leptonic $t\bar{t}$. Estimated using data-driven method
- Electron charge misidentification background: From Z and dileptonic $t\bar{t}$.
- Other backgrounds: $V\gamma$ (2.4%), ZZ , $t\bar{t}V$, VVV (total 1.6%)

Uncertainties with Significant Impact:

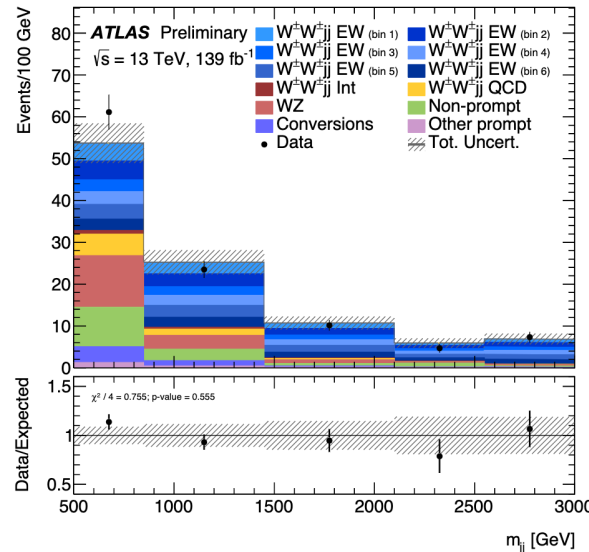
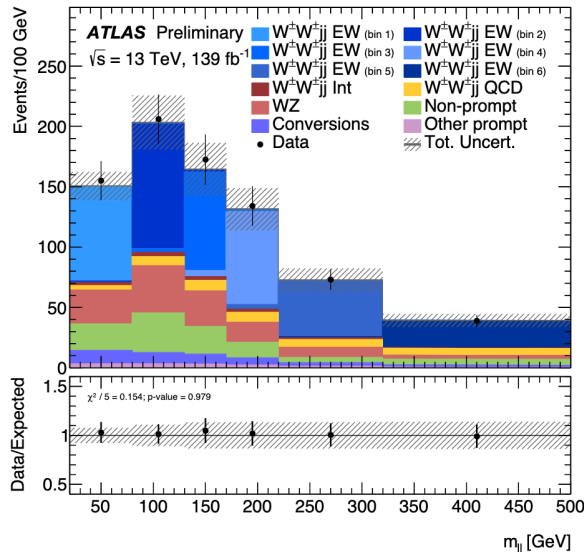
- Experimental: 6.7% (Misidentified Lepton Bkg: 3.1%)
- Modelling: 7.4% (EW $W^\pm W^\pm jj$, QCD corrections: 3.5%, QCD $W^\pm W^\pm jj$ theory uncertainties: 2.3%)
- Statistical: 7.4%
- Total: 10%

(Same sign) $W^\pm W^\pm jj$ Cross-section Measurement

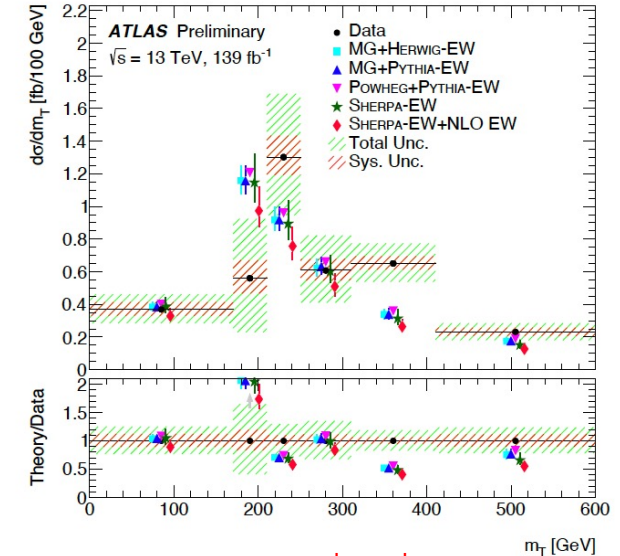
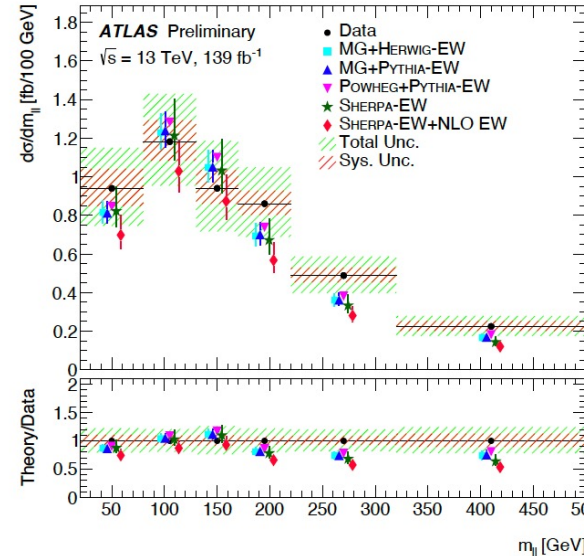
- Fiducial Cross-section measurement: Fiducial region defined as close to analysis signal region and detector acceptance as possible.
 - Signal region split in 4 regions according to the lepton flavors in the final state

Description	$\sigma_{\text{fid}}^{\text{EW}}$, fb	$\sigma_{\text{fid}}^{\text{EW+Int+QCD}}$, fb
Measured cross section	2.88 ± 0.21 (stat.) ± 0.19 (syst.)	3.35 ± 0.22 (stat.) ± 0.20 (syst.)
MG_AMC@NLO+HERWIG	2.53 ± 0.04 (PDF) $\pm_{0.19}^{0.22}$ (scale)	2.93 ± 0.05 (PDF) $\pm_{0.27}^{0.34}$ (scale)
MG_AMC@NLO+PYTHIA	2.55 ± 0.04 (PDF) $\pm_{0.19}^{0.22}$ (scale)	2.94 ± 0.05 (PDF) $\pm_{0.27}^{0.33}$ (scale)
SHERPA	2.44 ± 0.03 (PDF) $\pm_{0.27}^{0.40}$ (scale)	2.80 ± 0.03 (PDF) $\pm_{0.36}^{0.53}$ (scale)
POWHEG BOX +PYTHIA	2.67	—

- Likelihood based unfolding.
- P-values range from 0.014 to 0.623 across five variables used showing good Data-MC agreement.



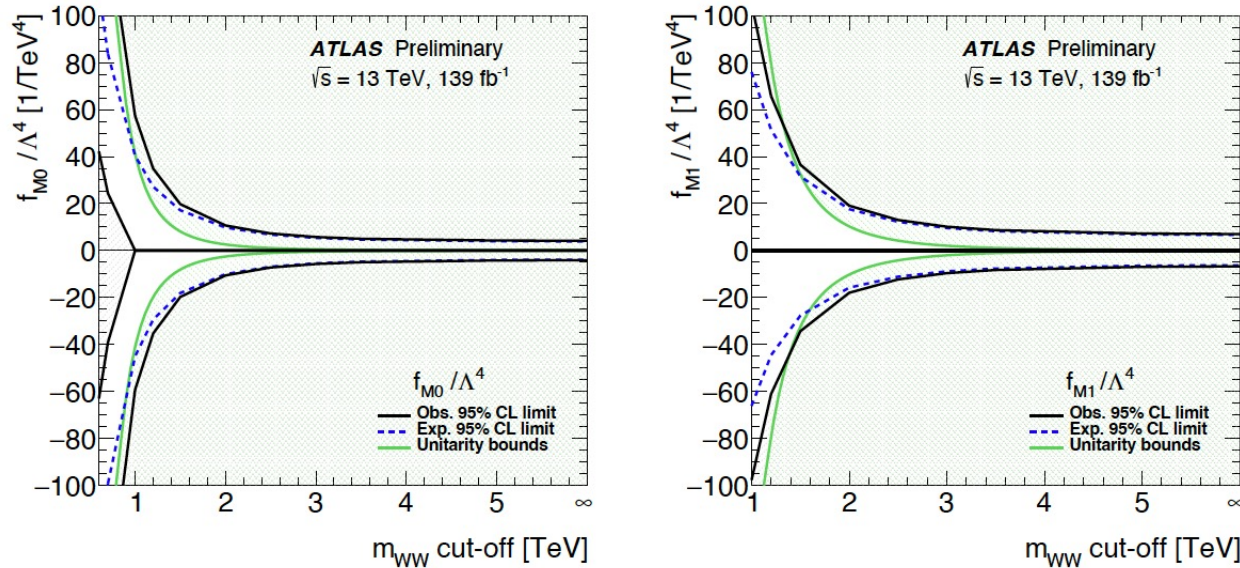
Post-fit distributions of $m_{\ell\ell}$ and m_{jj} for fiducial cross-section measurement



Fiducial differential cross sections of EW $W^\pm W^\pm jj$ production as a function of $m_{\ell\ell}$ and m_T .

(Same sign) $W^\pm W^\pm jj$ EFT Interpretations

- Maximum likelihood fits are performed by keeping other coefficients to zero and maximizing the likelihood with respect to the nuisance parameters.
- The 95% CLs are calculated on the Wilson Coefficients for dimension-8 operators with and without unitary bounds.



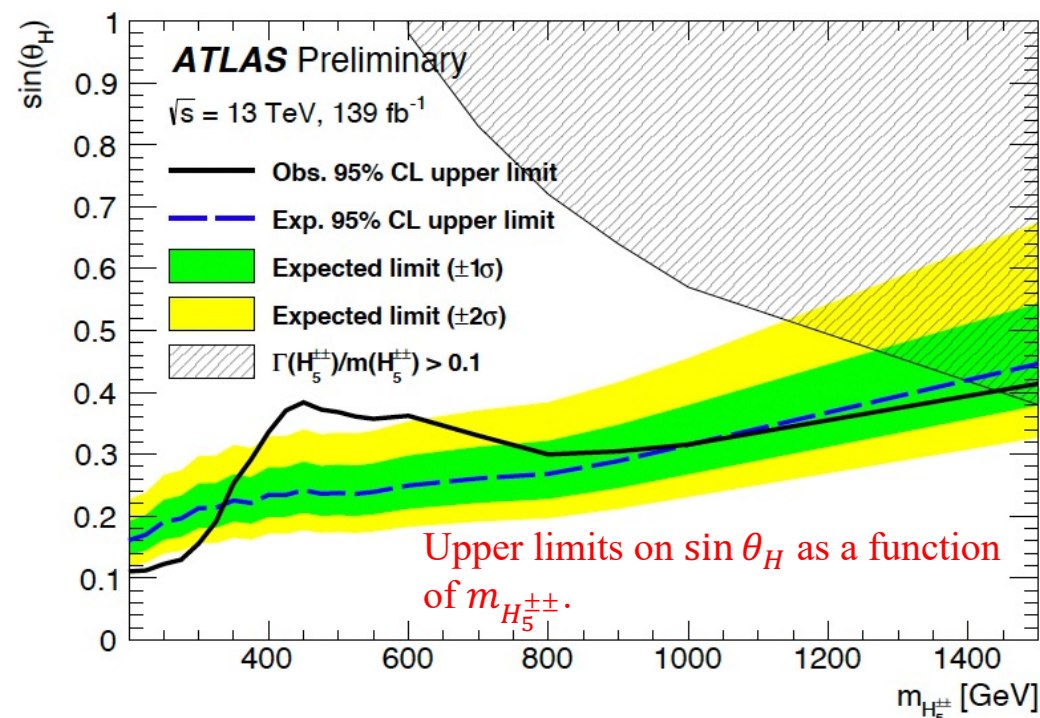
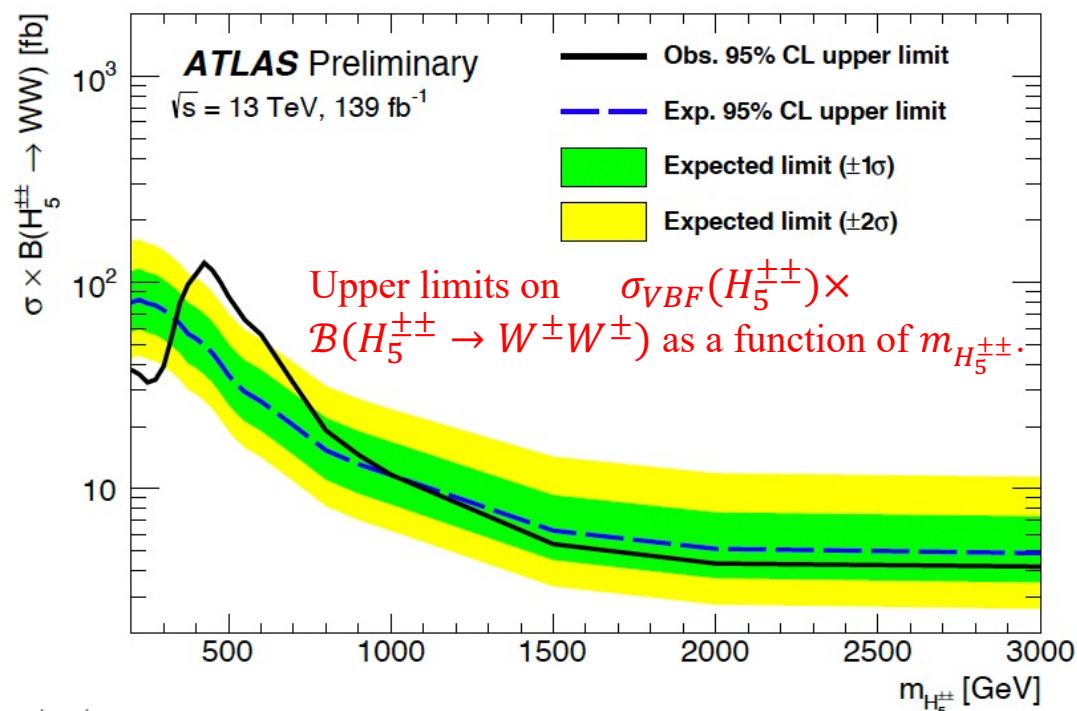
Limits at 95% CL as a function of the cut-off scale

Coefficient	Type	No unitarisation cut-off [TeV ⁻⁴]	Lower and upper limit at the respective unitarity bound [TeV ⁻⁴]
f_{M0}/Λ^4	exp.	[-3.9, 3.8]	-64 at 0.9 TeV, 40 at 1.0 TeV
	obs.	[-4.1, 4.1]	-140 at 0.7 TeV, 117 at 0.8 TeV
f_{M1}/Λ^4	exp.	[-6.3, 6.6]	-25.5 at 1.6 TeV, 31 at 1.5 TeV
	obs.	[-6.8, 7.0]	-45 at 1.4 TeV, 54 at 1.3 TeV
f_{M7}/Λ^4	exp.	[-9.3, 8.8]	-33 at 1.8 TeV, 29.1 at 1.8 TeV
	obs.	[-9.8, 9.5]	-39 at 1.7 TeV, 42 at 1.7 TeV
f_{S02}/Λ^4	exp.	[-5.5, 5.7]	-94 at 0.8 TeV, 122 at 0.7 TeV
	obs.	[-5.9, 5.9]	-
f_{S1}/Λ^4	exp.	[-22.0, 22.5]	-
	obs.	[-23.5, 23.6]	-
f_{T0}/Λ^4	exp.	[-0.34, 0.34]	-3.2 at 1.2 TeV, 4.9 at 1.1 TeV
	obs.	[-0.36, 0.36]	-7.4 at 1.0 TeV, 12.4 at 0.9 TeV
f_{T1}/Λ^4	exp.	[-0.158, 0.174]	-0.32 at 2.6 TeV, 0.44 at 2.4 TeV
	obs.	[-0.174, 0.186]	-0.38 at 2.5 TeV, 0.49 at 2.4 TeV
f_{T2}/Λ^4	exp.	[-0.56, 0.70]	-2.60 at 1.7 TeV, 10.3 at 1.2 TeV
	obs.	[-0.63, 0.74]	-

- Limits at 95% confidence level (CL) are extracted, including their effects both on EW $W^\pm W^\pm jj$ and EW $W^\pm Zjj$ ([ATL-PHYS-PUB-2023-002](#)).
- Including the effect of the EFT operators on the EW $W^\pm Zjj$ production, the limits improve by ~1-4%.

(Same sign) $W^\pm W^\pm jj$ Search for Doubly Charged Higgs

- Model independent upper limits calculated on $\sigma_{VBF}(H_5^{\pm\pm}) \times \mathcal{B}(H_5^{\pm\pm} \rightarrow W^\pm W^\pm)$.
- Also interpreted in the context of the Georgi–Machacek (GM) model giving upper limit on $\sin \theta_H$ parameter (characterises the contribution of the isotriplet scalar fields to the masses of the W and Z bosons) as a function of $m_{H_5^{\pm\pm}}$.
- These exclude parameter values greater than 0.11-0.41 for the $m_{H_5^{\pm\pm}}$ range of 200 to 1500 GeV.
- They show a local excess at a resonance mass of around 450 GeV with local significance of 3.2σ and global significance of 2.5σ .



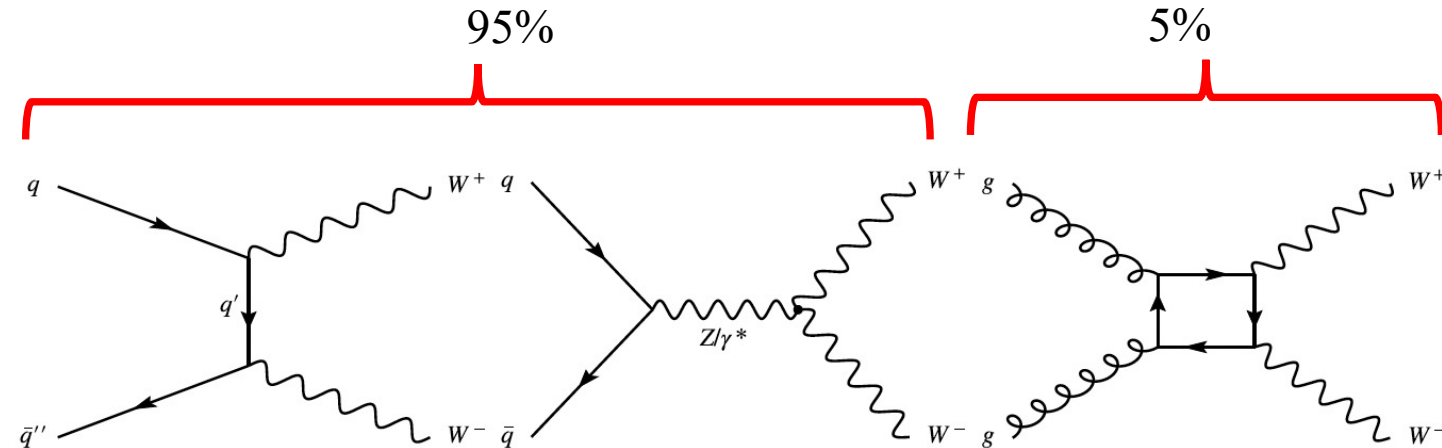
3

(Opposite Sign) W^+W^- Cross-section Measurement

- W^+W^- cross-section measurement is performed without any requirements on the jets (first jet-inclusive measurement). This allows for precise comparison with theory.
- Using integrated luminosity of 140 fb^{-1} .
- Fully leptonic final state with different flavor opposite charge leptons: $W^\pm W^\mp \rightarrow e^\pm \nu \mu^\mp \bar{\nu}$

Event Selection:

- Exactly two opposite charge leptons: one electron and one muon
- No additional lepton with $p_T > 10 \text{ GeV}$.
- 0 b-jets
- $m_{\ell\ell'} > 85 \text{ GeV}$



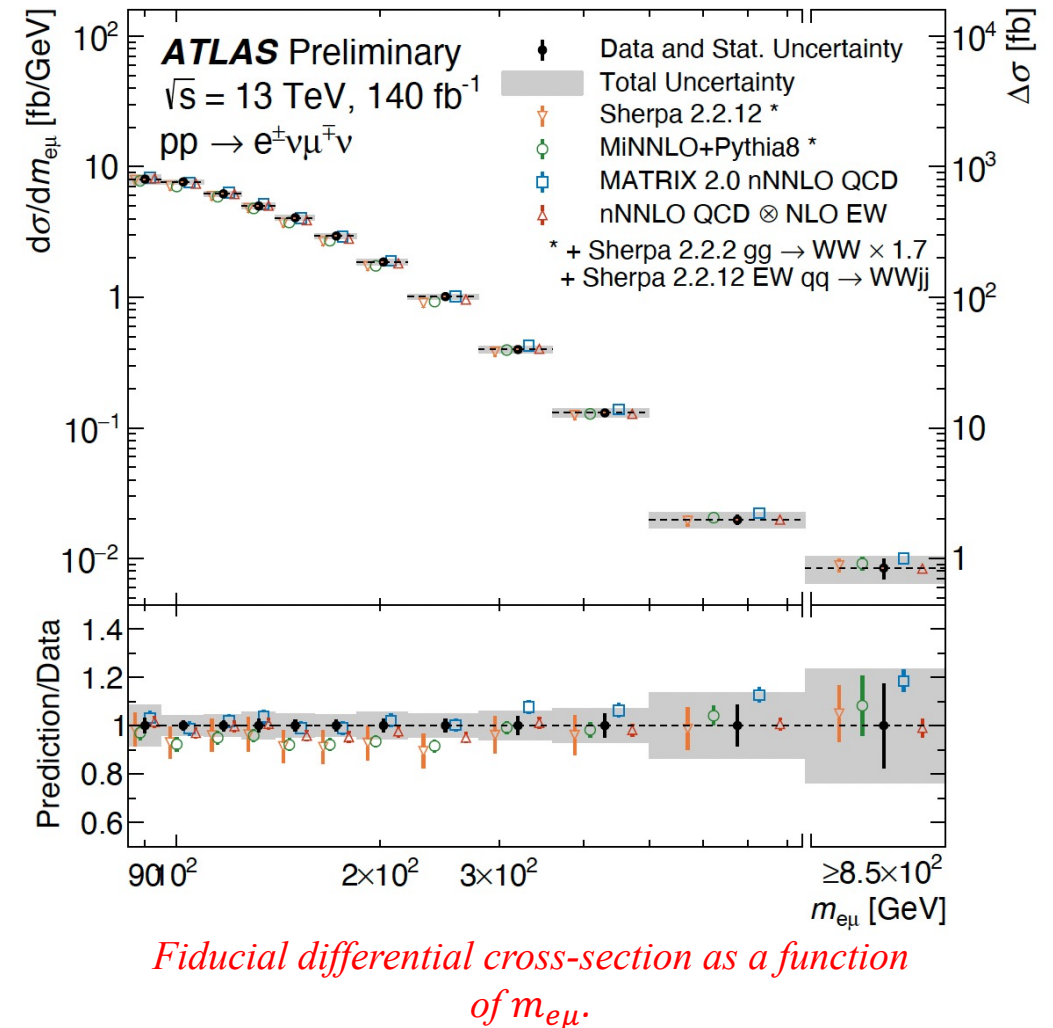
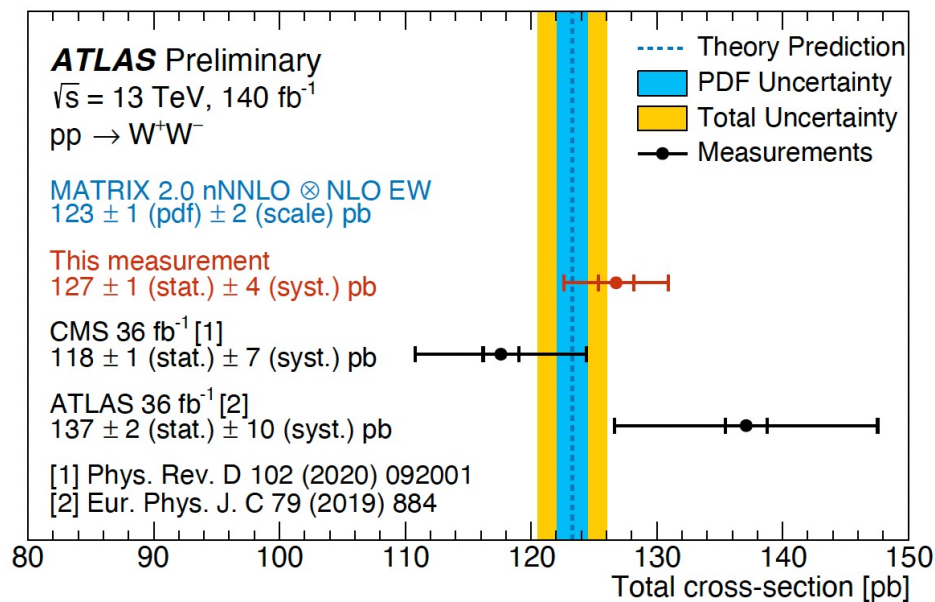
Backgrounds:

- 60% of all events is background
 - $t\bar{t}$ or single top Wt (80% of the total background)
- Other backgrounds: Z +jets production, events with non-prompt or misidentified leptons, and diboson production (WZ , $W\gamma$, ZZ , and $Z\gamma$).

(Opposite Sign) W^+W^- Cross-section Measurement

- The fiducial integrated and differential cross-section measurements with 12 observables (in backup):
 - The fiducial cross-section extrapolated to the total cross-section measurement:

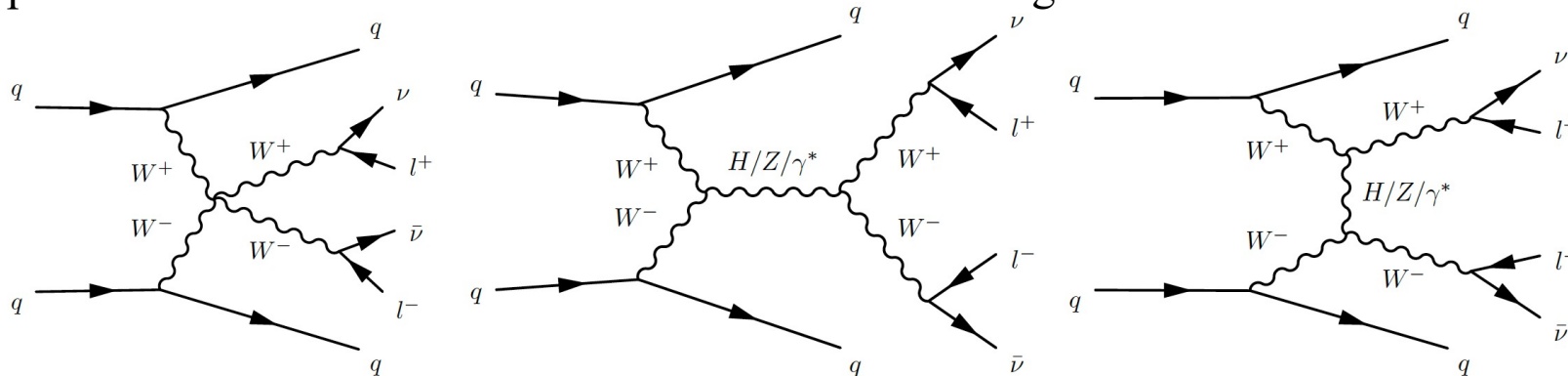
$$127 \pm 1 \text{ (stat.)} \pm 4 \text{ (syst.) pb}$$
- Improved data-driven estimates of top and fake backgrounds reduce uncertainty in the fiducial region to 3.1%.



(Opposite Sign) Electroweak Production of W^+W^-jj

Electroweak Production of (opposite sign) W^+W^- associated with jets.

Fully leptonic, opposite flavor oppositely charged leptons are selected: $W^\pm W^\mp jj \rightarrow e^\pm \nu \mu^\mp \bar{\nu} jj$. This has enhanced sensitivity compared to the same flavor channel. Low Drell-Yan Background.



Event Selection:

- Signal process tends to produce events with positive lepton centrality.
 - Centrality $\zeta = \min\{\min(\eta_{\ell_1}, \eta_{\ell_2}) - \min(\eta_{j_1}, \eta_{j_2}), [\max(\eta_{j_1}, \eta_{j_2}) - \max(\eta_{\ell_1}, \eta_{\ell_2})]\} > 0.5$.
 - The Signal to background ratio is enhanced with this cut.
- $m_{e\mu} > 80$ GeV
- $E_T^{miss} > 15$ GeV
- No b -jets

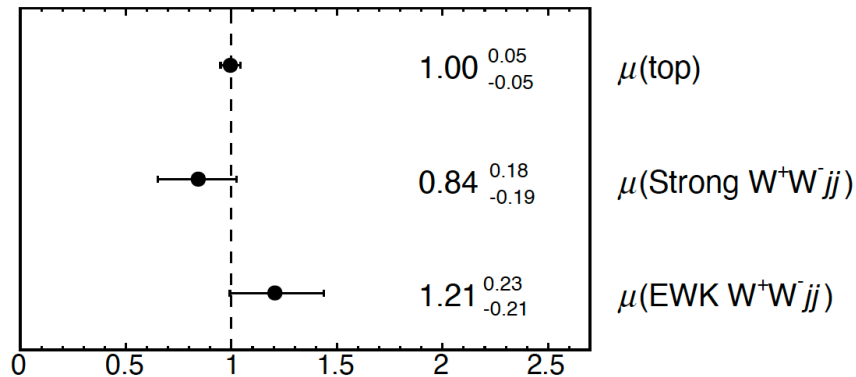
Backgrounds:

- Top background: 66% of the inclusive region. Modelled using simulation and constrained using data in a dedicated CR.
- Strong production of W^+W^-jj : 24% of the inclusive region
- $Z + jets$ (4%)
- Multiboson (2%)
- $W + jets$ where one jet is mis-identified as a lepton (below 1%).

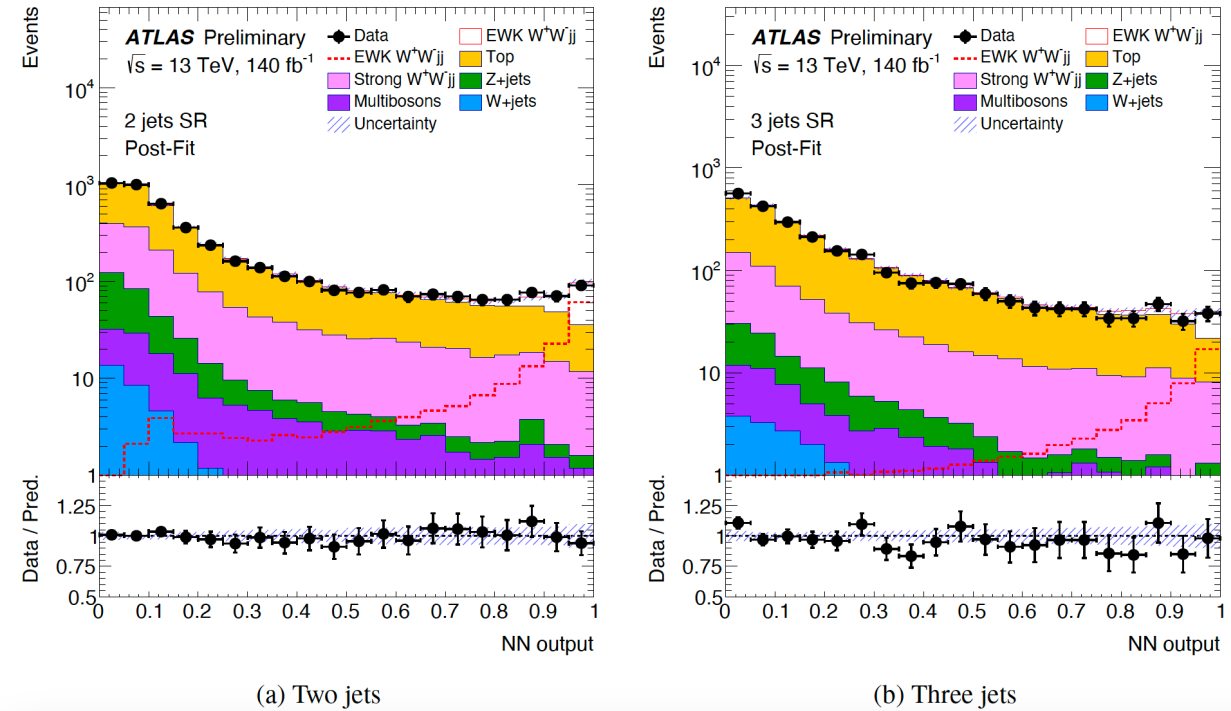
(Opposite Sign) EW W^+W^-jj : Signal Extraction and Cross-section Measurement

- The Signal and other SM processes are separated using a Neural Network. The backgrounds considered are the dominant top quark and strong W^+W^- processes as backgrounds
- Output is between 0 (background-like) and 1 (signal-like)
- The Neural Network is trained for 2 jets and 3 jets categories separately.

ATLAS Preliminary $\sqrt{s} = 13 \text{ TeV}, 140 \text{ fb}^{-1}$



Signal strengths as floating parameters for background and signal processes



NN output distribution in the signal region (SR)

Results:

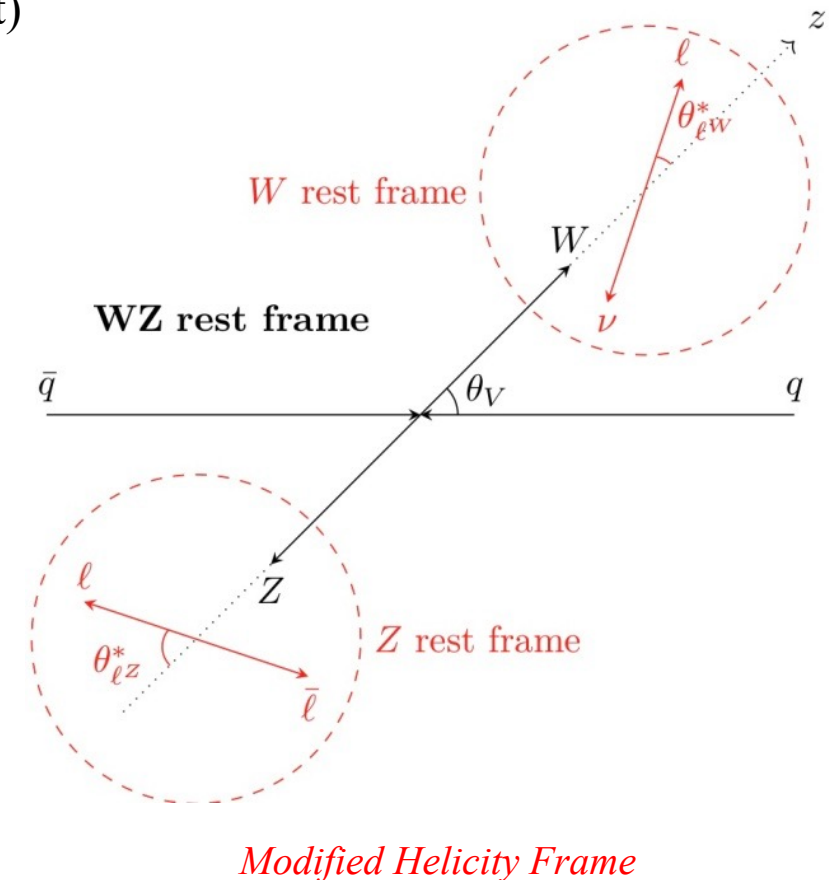
- The Signal has been observed with an observed (expected) significance of 7.1σ (6.2σ).
- Cross section in a signal-enriched fiducial volume $2.65^{+0.52}_{-0.48} \text{ fb}$ (Powheg Box predictor $2.20^{+0.14}_{-0.13} \text{ fb}$).
- Dominant uncertainty comes from the data statistics.

$W^\pm Z$ Polarization Studies in ATLAS

- **First-ever observation of longitudinal-longitudinal joint polarization state in diboson production.**
- Experimental Signature: $p p \rightarrow \ell \bar{\ell} \ell' \nu_{\ell'} + X$
- Inclusive Fiducial phase space for cross-section measurement and joint and single polarization fraction extraction
- Modified Helicity frame used for defining polarization (not Lorentz Invariant)
- p_Z^ν reconstruction: New DNN-based method.
 - Reasonable p_Z^ν estimate for which analytical method fails
 - 10% decrease in RMS due to improved p_Z^ν resolution.

Backgrounds:

- **Irreducible background** (all candidates are prompt or from τ -lepton) 18%:
 - Using MC samples
 - ZZ – 7.5%, Main background (QCD+EW)
 - ttV : 4%
 - $WZ \rightarrow \tau \ell \ell \rightarrow \ell \nu \ell \ell$: 3%
 - Others: $t + Z$, triboson VVV , VBS WZ , $W^\pm \gamma^*$ produced outside of total phase space.
- **Reducible background** (at least one non-prompt lepton):
 - Using data-driven method
 - Misidentified leptons: $Z + \gamma$, $t\bar{t}$, Z +jets



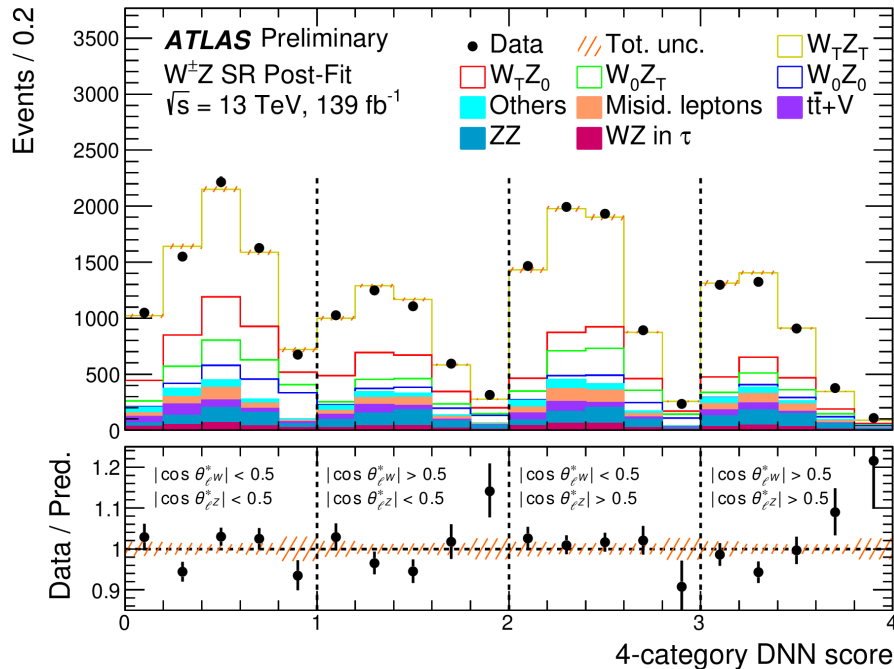
Modified Helicity Frame

$W^\pm Z$: Polarization Templates

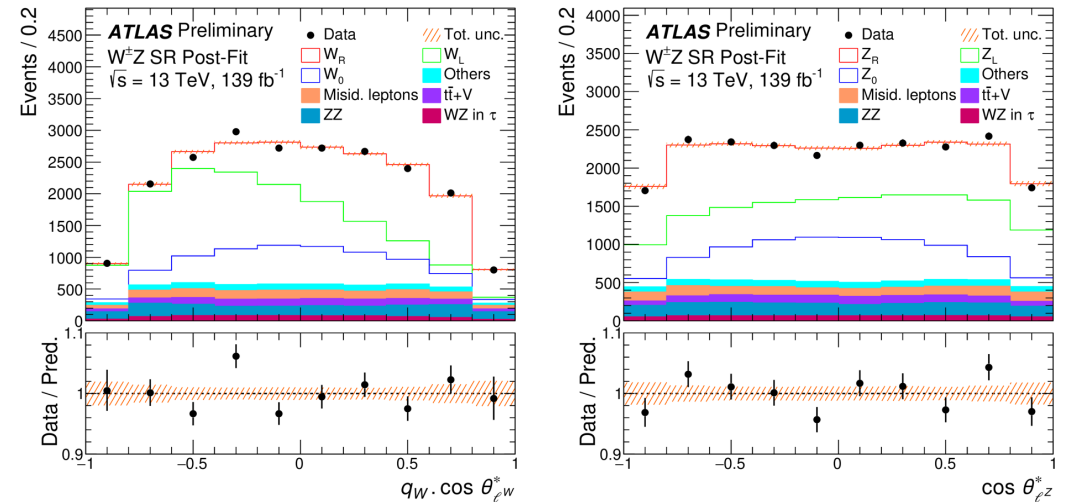
Joint Polarization:

- Polarized samples are produced at LO with $WZ+0,1$ jets.
- NLO-accurate polarization templates are required.
- 4 Categories were used for training 4 DNNs.
- Many validations are done to get NLO-accurate templates using LO polarized samples.

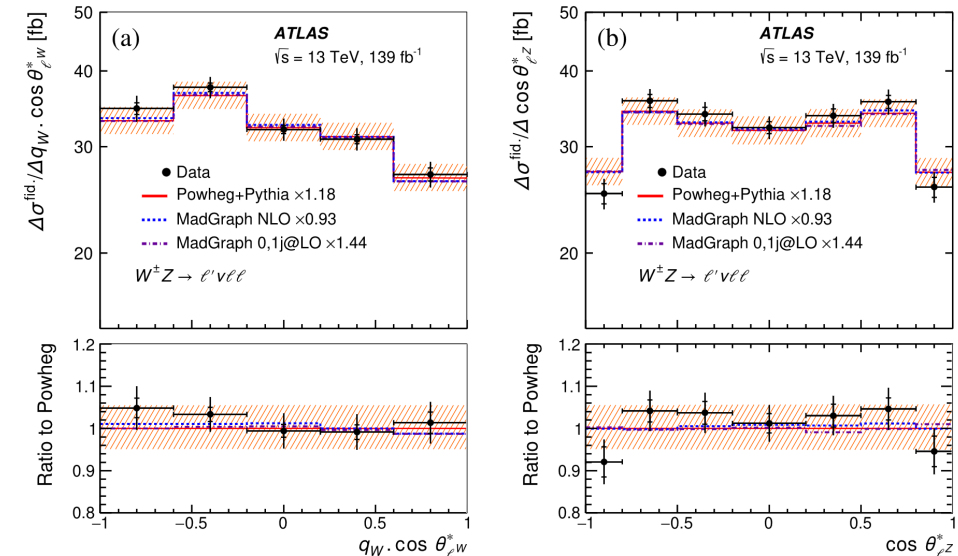
Single Polarization templates using analytical reweighting: Agreement of fitted templates with



DNN Score distributions in 4 categories



Iterative Bayesian unfolding for differential cross-section measurements in the fiducial phase space.



$W^\pm Z$ Polarization Fractions Results

Joint Polarization:

- First ever observation of $V_0 V_0$.

Fraction	Significance: Observed (Expected)
f_{00}	7.1σ (6.2σ)
f_{0T}	3.4σ (5.4σ)
f_{T0}	7.1σ (6.6σ)
f_{TT}	11σ (9.7σ)

	Data	POWHEG+PYTHIA	NLO QCD
$W^\pm Z$			
f_{00}	0.067 ± 0.010	0.0590 ± 0.0009	0.058 ± 0.002
f_{0T}	0.110 ± 0.029	0.1515 ± 0.0017	0.159 ± 0.003
f_{T0}	0.179 ± 0.023	0.1465 ± 0.0017	0.149 ± 0.003
f_{TT}	0.644 ± 0.032	0.6431 ± 0.0021	0.628 ± 0.004
$W^+ Z$			
f_{00}	0.072 ± 0.016	0.0583 ± 0.0012	0.057 ± 0.002
f_{0T}	0.119 ± 0.034	0.1484 ± 0.0022	0.155 ± 0.003
f_{T0}	0.153 ± 0.033	0.1461 ± 0.0022	0.147 ± 0.003
f_{TT}	0.66 ± 0.04	0.6472 ± 0.0026	0.635 ± 0.004
$W^- Z$			
f_{00}	0.063 ± 0.016	0.0600 ± 0.0014	0.059 ± 0.002
f_{0T}	0.11 ± 0.04	0.1560 ± 0.0027	0.166 ± 0.003
f_{T0}	0.21 ± 0.04	0.1470 ± 0.0027	0.152 ± 0.003
f_{TT}	0.62 ± 0.05	0.6370 ± 0.0033	0.618 ± 0.004

Single Polarization:

	f_0			$f_L - f_R$		
	Data	POWHEG+PYTHIA	NLO QCD	Data	POWHEG+PYTHIA	
W in $W^+ Z$	0.23 ± 0.05	0.2044 ± 0.0024	0.211 ± 0.002	0.071 ± 0.023	0.0990 ± 0.0015	
W in $W^- Z$	0.19 ± 0.05	0.217 ± 0.004	0.225 ± 0.001	0.026 ± 0.027	-0.0491 ± 0.0020	
W in $W^\pm Z$	0.22 ± 0.04	0.2094 ± 0.0016	0.217 ± 0.001	0.059 ± 0.016	0.0390 ± 0.0011	
Z in $W^+ Z$	0.223 ± 0.025	0.1971 ± 0.0019	0.206 ± 0.002	-0.20 ± 0.10	-0.217 ± 0.006	
Z in $W^- Z$	0.240 ± 0.029	0.2065 ± 0.0023	0.211 ± 0.001	0.10 ± 0.13	0.092 ± 0.007	
Z in $W^\pm Z$	0.231 ± 0.019	0.2009 ± 0.0014	0.208 ± 0.001	-0.10 ± 0.08	-0.092 ± 0.005	

- Here the NLO QCD predictions are from Denner&Pelliccioli [[arXiv:2010.07149](https://arxiv.org/abs/2010.07149)]

- Better than 2σ agreement for joint polarization fractions.
- f_0 agrees within 1σ
- $f_L - f_R$ agrees within 1.5σ , except $W^- Z$ (2.8σ)

Spin-correlations between longitudinal W and Z:

- Measured $R_c = f_{00} / (f_0^W f_0^Z) = 1.54 \pm 0.35$ (Obs. Significance 1.6σ wrt $R_c = 1$ hypothesis)
- Predicted (NLO QCD) $R_c = 1.3$.

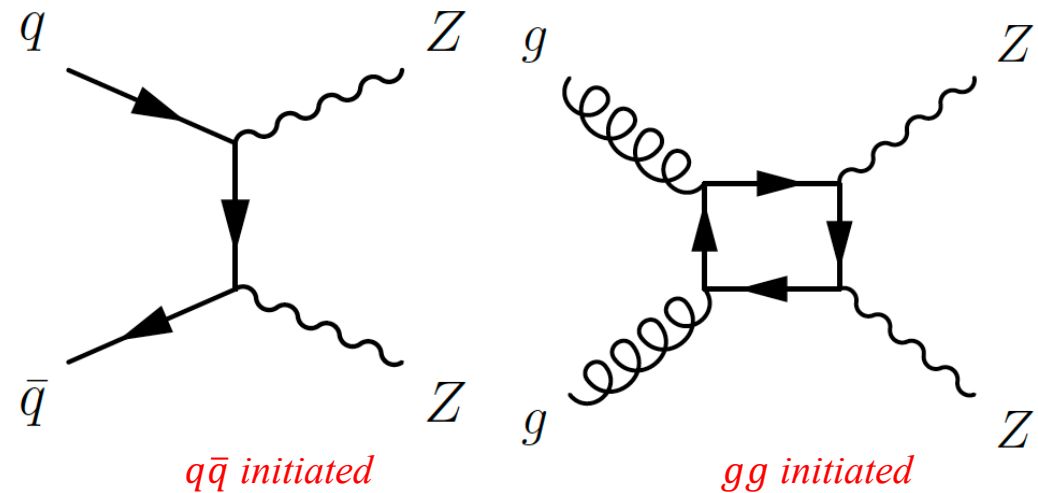
Cross-section in inclusive fiducial phase space (also measured differentially):

- Measured: $\sigma_{W^\pm Z \rightarrow \ell' \nu \ell \ell}^{fid} = 64.6 \pm 2.1$ fb
- NNLO Expectation: $\sigma_{W^\pm Z \rightarrow \ell' \nu \ell \ell}^{fid} = 64.0_{-1.3}^{+1.5}$ fb

ZZ Polarization and CP Property Measurement

[ATLAS-CONF-2023-038](#)

- **Measurement of $Z_L Z_L$** (both longitudinally polarized). Helps probing the EWSB and new physics searches.
- **Measurement of CP-sensitive observables** in diboson production for exploring new sources of CP violation.
- In this analysis, unfolded differential cross-section measured for an Optimal Observable (OO). Results are interpreted to constrain aNTGC using an effective vertex function approach. aNTGC vertex can be parameterised with two coupling parameters f_Z^4 and f_γ^4 that violate CP symmetry.
- Fully leptonic final states: $ZZ \rightarrow \ell^+ \ell^- \ell'^+ \ell'^-$, the leptons can be electron or muon (SFOC leptons).
- possible combinations SFOC pairs + invariant mass of Z constraint.
- $m_{4\ell} > 180$ GeV.

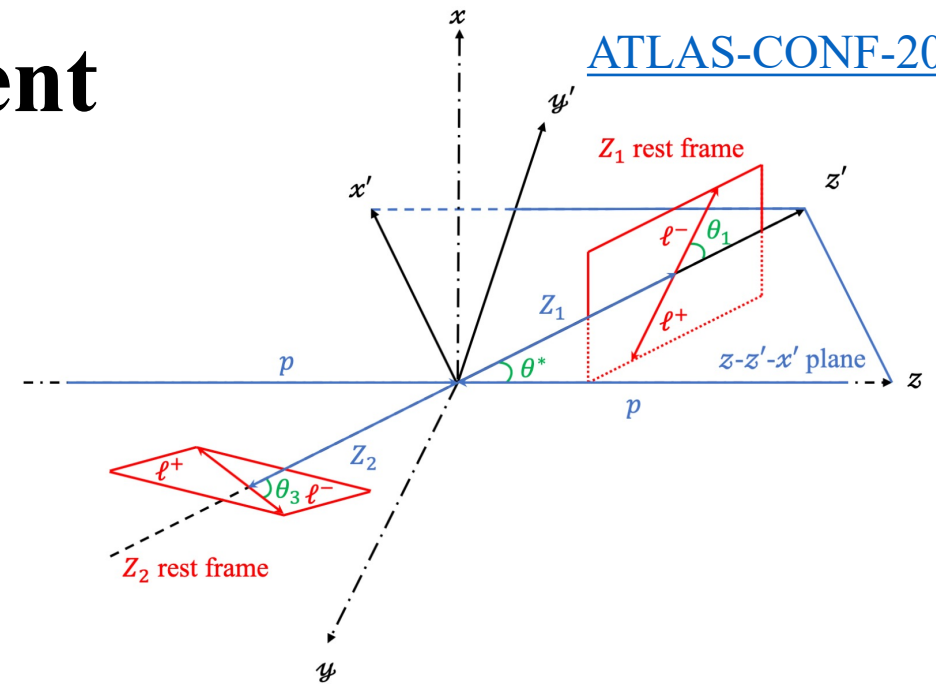


Backgrounds:

- Reducible (8-9% of $Z_L Z_L$ events): non-prompt leptons from hadron decays, charge misidentification, or photon conversion. Fake-factor determination done using Z +jets and $t\bar{t}$ CR.
- Irreducible (9-10% of $Z_L Z_L$ events): $t\bar{t}Z, VVZ$.

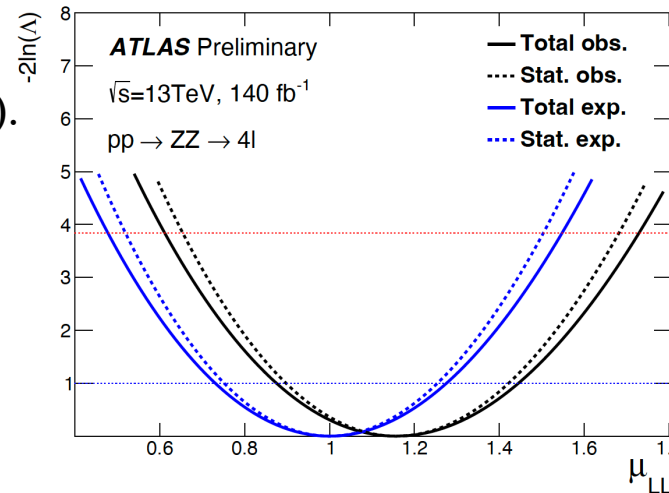
$Z_L Z_L$: Cross-section Measurement

- For the extraction of $Z_L Z_L$ cross-section, multivariate technique based on Boosted Decision Trees (BDT).
- To reduce theoretical modelling uncertainties, only angular variables were used in BDT training.
- Higher order corrections, QCD+EW are applied. Theoretical calculations taken from [https://link.springer.com/article/10.1007/JHEP10\(2021\)097](https://link.springer.com/article/10.1007/JHEP10(2021)097).
 - 1D reweighting for each polarization
 - 1D reweighting for the interference effect
 - 2D reweighting for residual higher order corrections

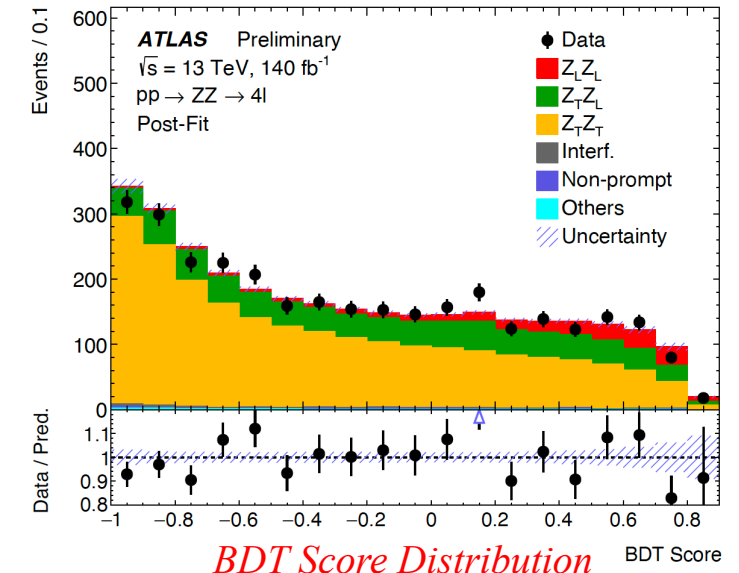


Results:

- Obs (exp) significance of 4.3σ (3.8σ).
- An additional likelihood fit is performed to convert signal strength to cross-section:
- Obs: $\sigma_{Z_L Z_L}^{obs.} = 2.44 \pm 0.59 fb$
- SM Pred: $\sigma_{Z_L Z_L}^{pred.} = 2.09 \pm 0.10 fb$.



Likelihood Scan For Signal Strength



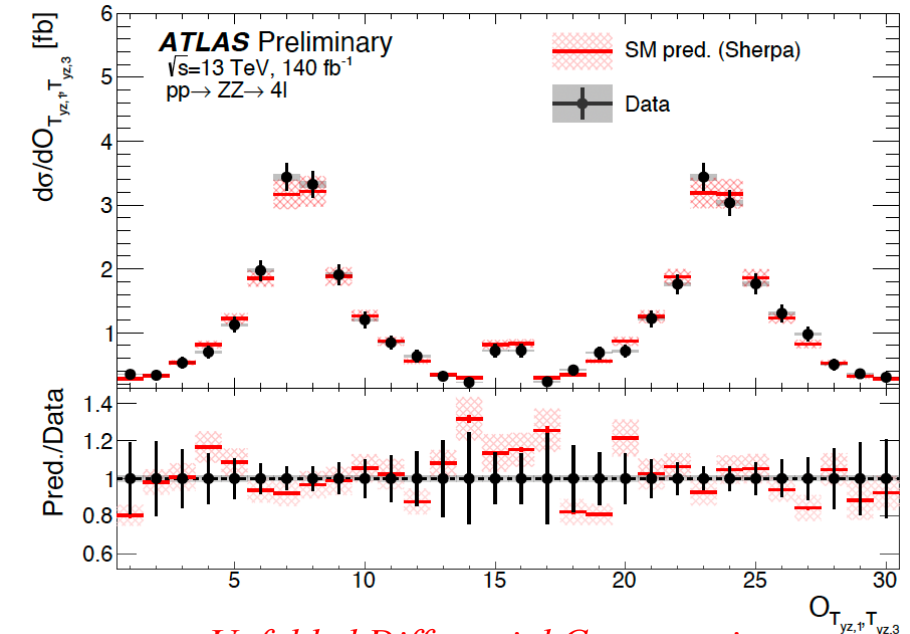
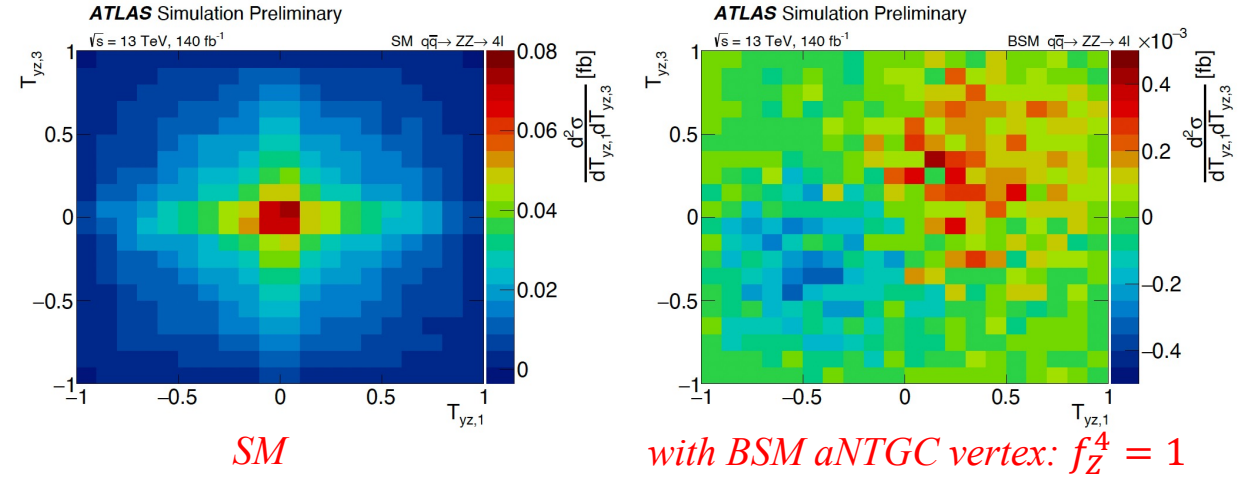
BDT Score Distribution

ZZ: Study of CP Property

- The differential cross-sections $\theta_1(\theta_3)$ and $\phi_1(\phi_3)$ are symmetric in the SM but asymmetric in the presence of the two CP-odd aNTGC. (1 and 3 correspond to the negatively charged leptons of the ZZ system).
- $\mathcal{O}_{T_{yz,1}, T_{yz,3}}$ defined from 2D distribution of T_{yz} by grouping sensitive and non-sensitive bins (here $T_{yz,1(3)} = \sin\phi_{1(3)} \times \cos\theta_{1(3)}$, maximizing asymmetry for each Z boson system).
- Miss-paired leptons have smaller impact on the CP sensitivity.
- The distributions are unfolded using the iterative Bayesian unfolding method.
- Exp and Obs 95% confidence intervals on CP-odd Operator:

$$\sigma^i = \sigma_{SM}^i + c \cdot \sigma_{interference}^i + c^2 \cdot \sigma_{quadratic}^i$$

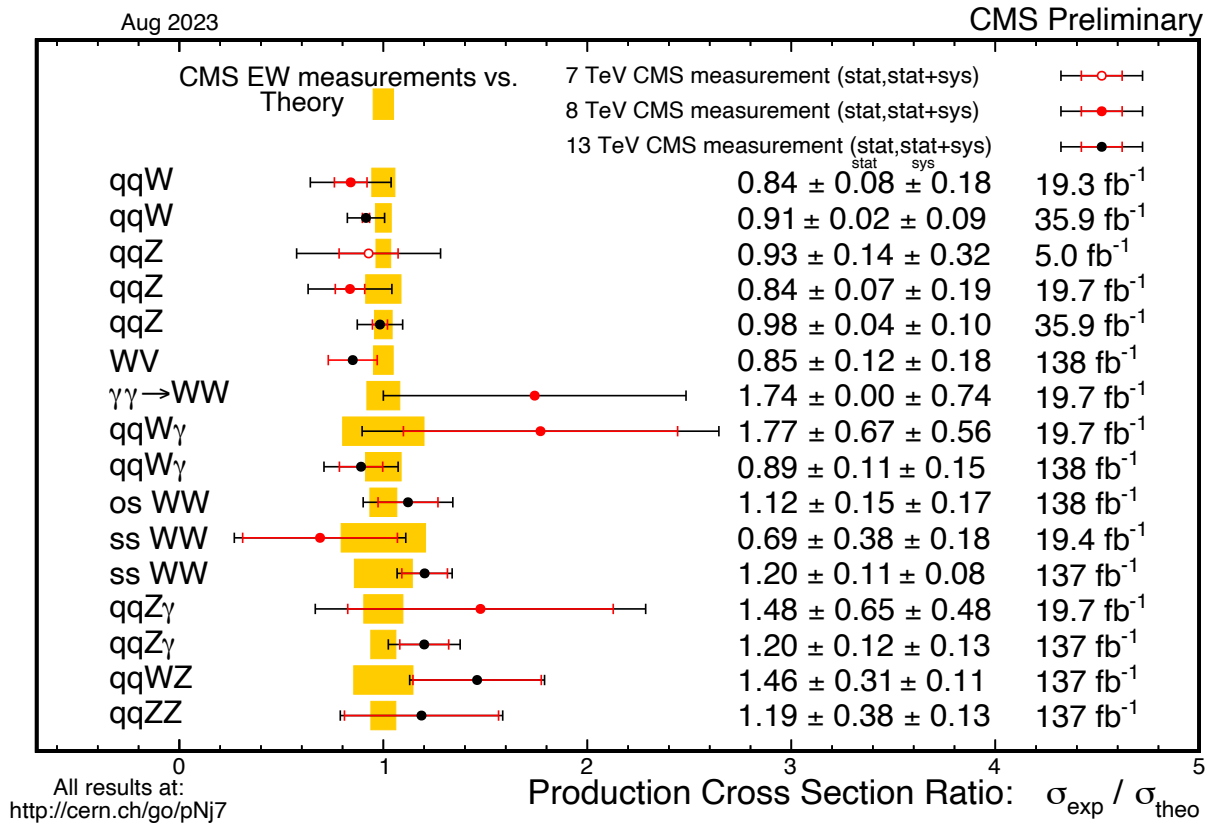
Xsec in a bin of CP sensitive observable



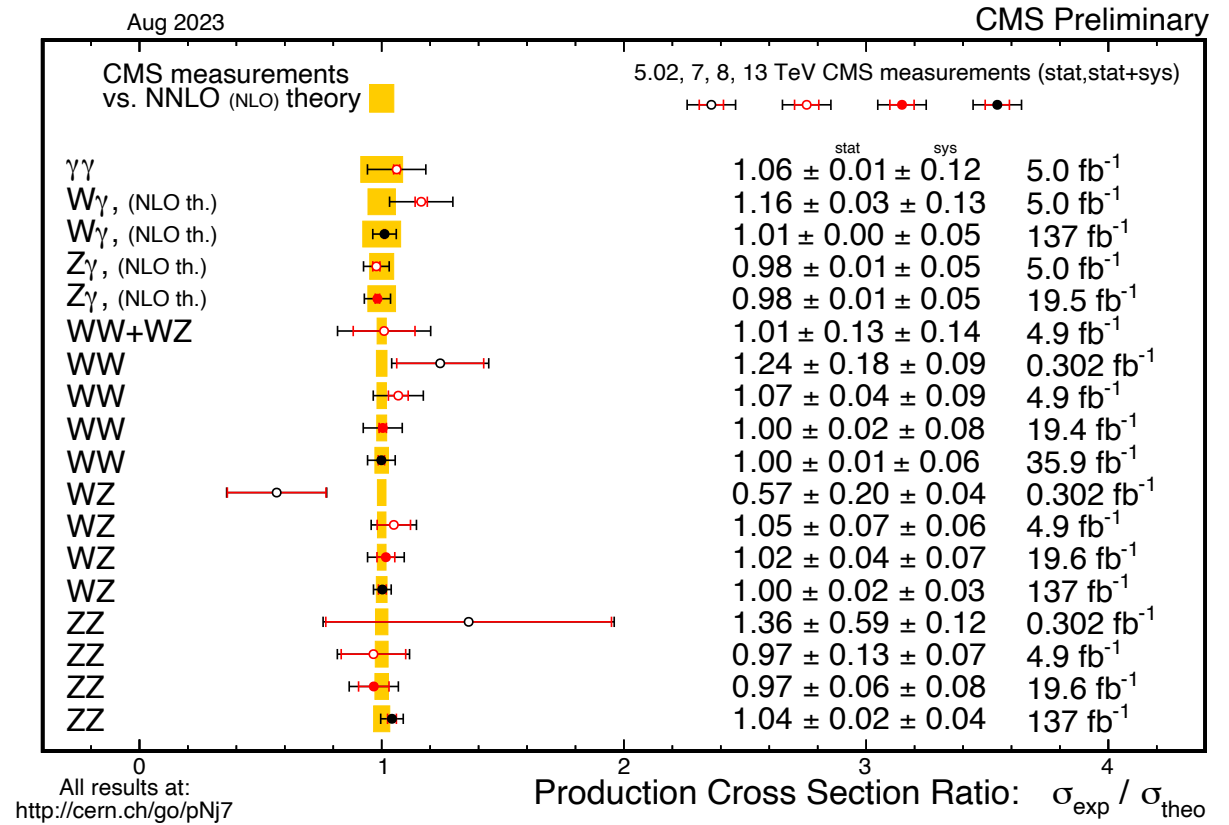
aNTGC parameter	Interference only		Full	
	Expected	Observed	Expected	Observed
f_Z^4	[-0.16, 0.16]	[-0.12, 0.20]	[-0.013, 0.012]	[-0.012, 0.012]
f_γ^4	[-0.30, 0.30]	[-0.34, 0.28]	[-0.015, 0.015]	[-0.015, 0.015]

Unfolded Differential Cross-section

Diboson Searches Summary: CMS



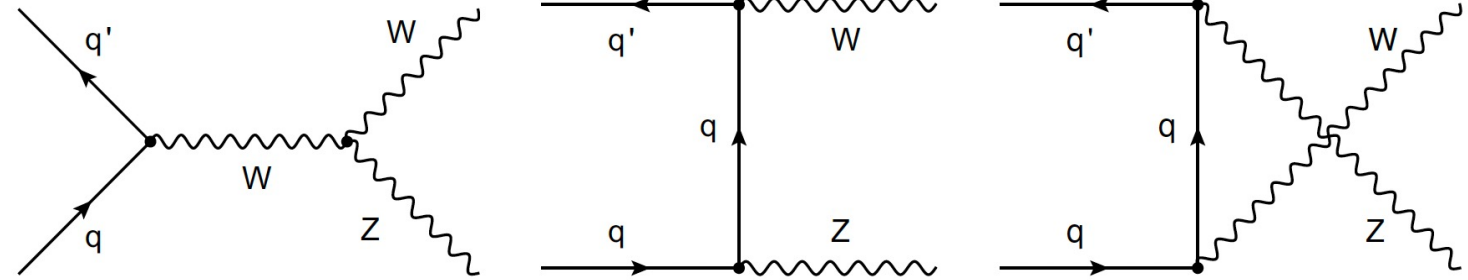
EW Diboson Cross-sections Vs Theory



Diboson Cross-sections Vs Theory

$W^\pm Z$ Introduction

- WZ is a dominant SM contribution to the triplepton final states, hence a background in many multileptonic final states
- Measurements performed:
 - inclusive cross section
 - charge asymmetry measurement
 - Boson polarization measurement
 - differential cross section
 - the search for anomalous triple gauge couplings



Event Selection:

- $N_\ell = 3$
- Number of opposite sign same flavor leptons ≥ 1 .
- $p_T^{miss} > 30 \text{ GeV}$
- No b-tagged jets
- $\min(M(\ell\ell')) > 4 \text{ GeV}$: For infrared safety and avoid contribution from low mass resonances.
- $M(\ell_{Z1}, \ell_{Z2}, \ell_W) > 100 \text{ GeV}$

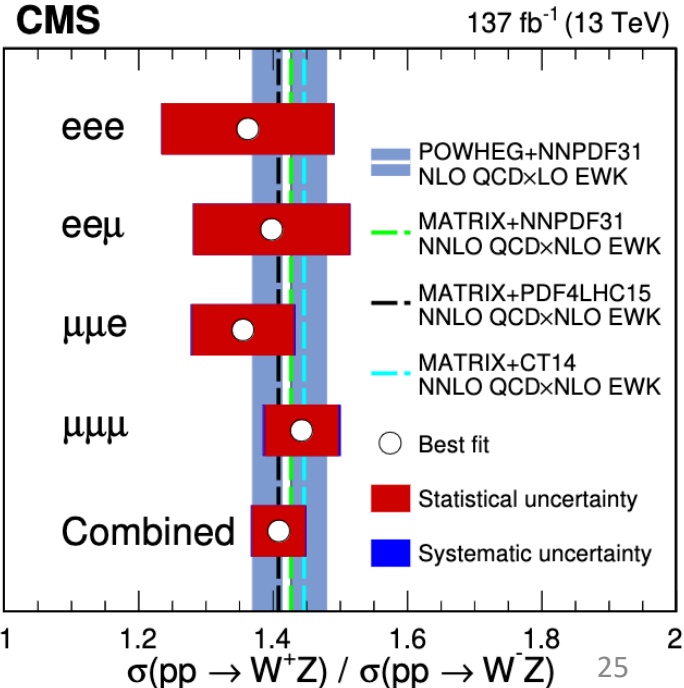
Backgrounds:

- Reducible: Estimated using right-to-loose data-driven method. Includes $Z + jets$ and $t\bar{t}$.
- Irreducible:
 - ZZ (6% of the SR yield), $t\bar{t}Z$ and tZq (3.2% of the SR yield), $X\gamma$ (1.5% of the total SR yield),

$W^\pm Z$ Cross-section Measurement

- Inclusive Cross-section measurement performed in flavour inclusive (combined) and in separate flavor categories ($eee, ee\mu, \mu\mu e, \mu\mu\mu$).
- Maximum likelihood fit is used for obtaining WZ yields in the SR.
 - $\sigma_{tot}(pp \rightarrow WZ) = 50.6 \pm 0.8 (stat) \pm 1.4 (syst) \pm 1.1 (lumi) \pm 0.5 (theo) pb$
- The normalization of the WZ process is kept as an unconstrained parameter in the fit for the cross-section measurement
- Charge asymmetry ratio is also measured (resulting from dominant qq' production): $A_{WZ}^{+-} = \frac{\sigma_{fid}(pp \rightarrow W^+Z)}{\sigma_{fid}(pp \rightarrow W^-Z)} = 1.41 \pm 0.04$.
- Consistency of the asymmetry ratio with different PDF sets is also calculated

Category or source	Total cross section
POWHEG	$42.5^{+1.6}_{-1.4} (scale) \pm 0.6 (PDF) pb$
MATRIX, NNLO QCD	$51.2^{+1.2}_{-1.0} (scale) pb$
MATRIX, NNLO QCD \times NLO EWK	$50.7^{+1.1}_{-1.0} (scale) pb$
eee (Measured)	$53.2 \pm 2.7 (stat) \pm 2.3 (syst) \pm 1.1 (lumi) \pm 0.5 (theo) pb$
$ee\mu$ (Measured)	$48.1 \pm 1.7 (stat) \pm 1.8 (syst) \pm 1.1 (lumi) \pm 0.4 (theo) pb$
$\mu\mu e$ (Measured)	$50.6 \pm 1.3 (stat) \pm 1.5 (syst) \pm 1.1 (lumi) \pm 0.5 (theo) pb$
$\mu\mu\mu$ (Measured)	$50.8 \pm 1.0 (stat) \pm 1.5 (syst) \pm 1.1 (lumi) \pm 0.5 (theo) pb$
Combined (Measured)	$50.6 \pm 0.8 (stat) \pm 1.5 (syst) \pm 1.1 (lumi) \pm 0.5 (theo) pb$



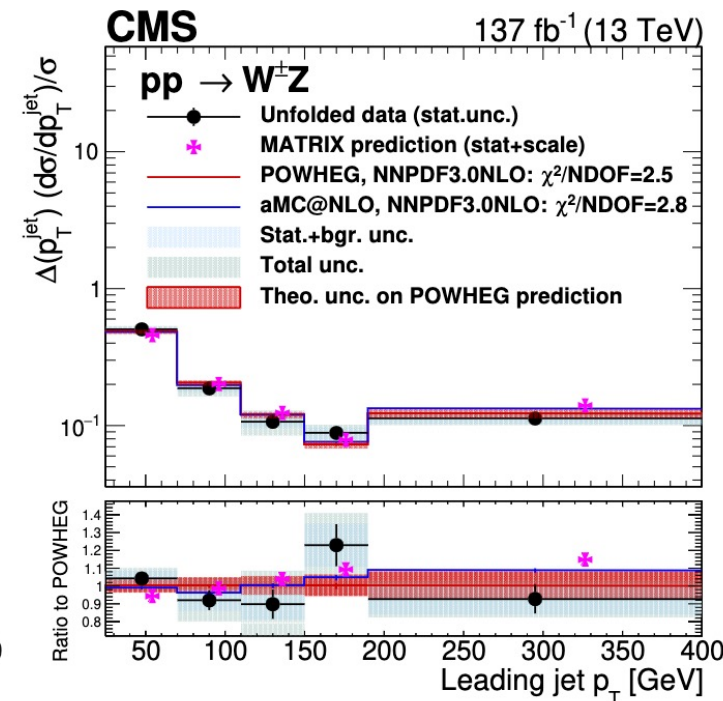
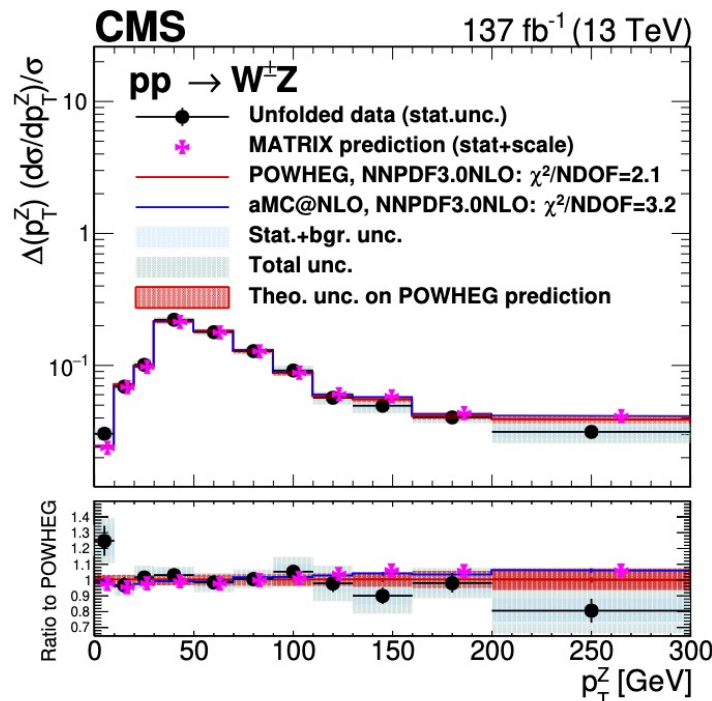
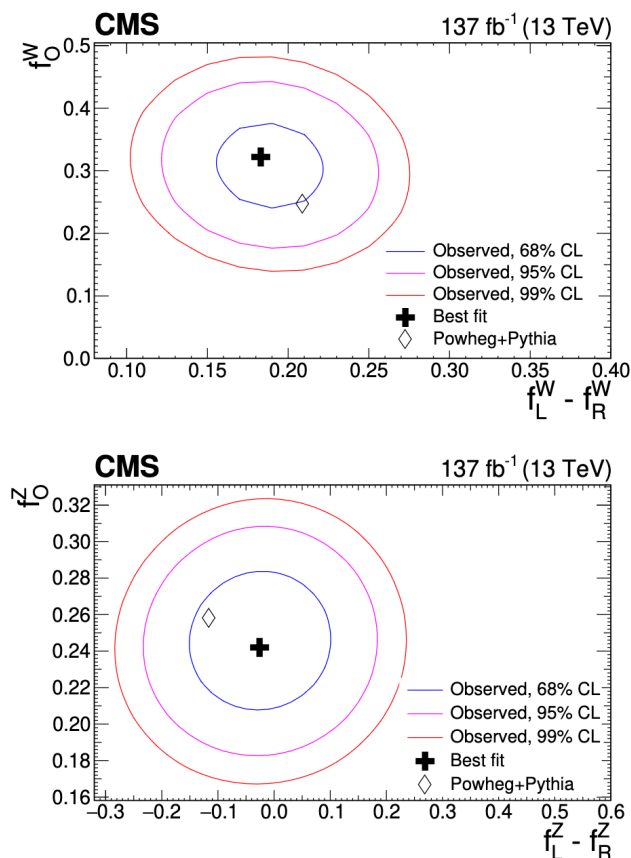
$W^\pm Z$ Polarization and Differential Cross-section

Single boson polarization measurement:

- Observation of longitudinally polarized W boson with obs (exp) significance of 5.6σ (4.3σ)
- Observation of longitudinal Z, obs and exp above 5σ .

Differential Cross-section measurement:

- based on a least squares fit as implemented in the TUnfold software package



$W^\pm Z$ aQGC Limits

- Anomalous couplings search is based on $M(WZ)$. Two different 95% confidence limits are set:
 - Both purely dimension-eight BSM contribution and dimension-six interference term are included to compute the EFT effect in the high tails of $M(WZ)$
 - Only dimension-six interference term is included
- Better than best previous limits
- Limits on three CP-conserving parameters ($c_{WWW}/\Lambda^2, c_W/\Lambda^2, c_b/\Lambda^2$) and two CP-violating parameters ($\tilde{c}_{WWW}/\Lambda^2, \tilde{c}_W/\Lambda^2$)

Parameter	95% CI, exp. (TeV^{-2})	95% CI, obs. (TeV^{-2})	Best fit, obs. (TeV^{-2})
c_w/Λ^2	$[-2.0, 1.3]$	$[-2.5, 0.3]$	-1.3
c_{www}/Λ^2	$[-1.3, 1.3]$	$[-1.0, 1.2]$	0.1
c_b/Λ^2	$[-86, 125]$	$[-43, 113]$	44
$\tilde{c}_{www}/\Lambda^2$	$[-0.76, 0.65]$	$[-0.62, 0.53]$	-0.03
\tilde{c}_w/Λ^2	$[-46, 46]$	$[-32, 32]$	0

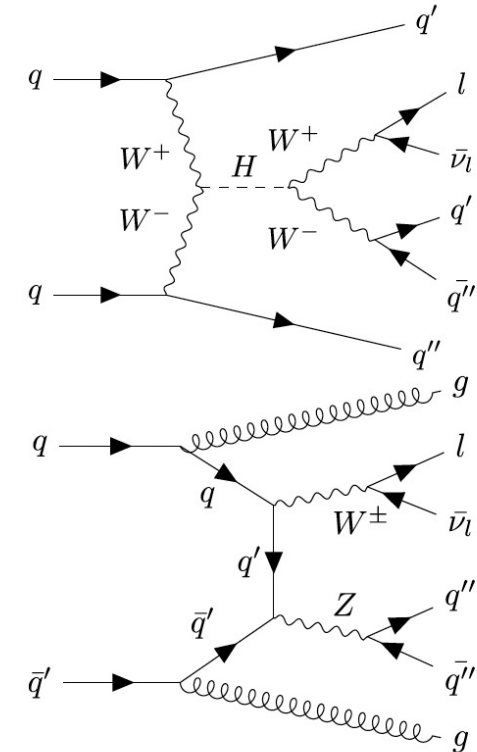
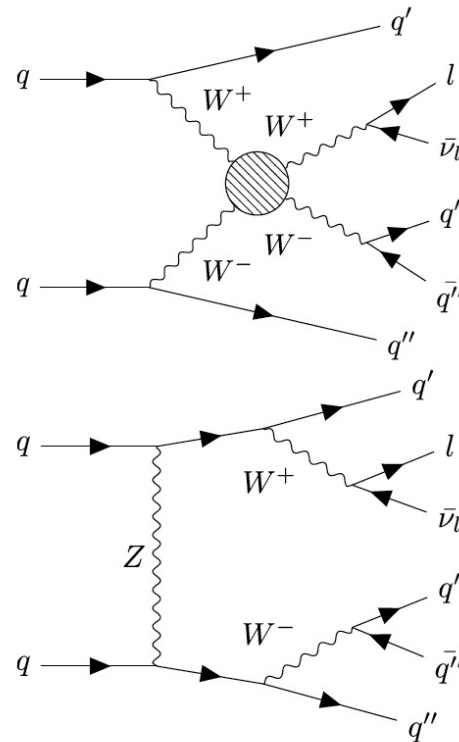
2

WVjj: Cross-section Measurements

- First LHC evidence of SM electroweak $\ell\nu qq$ production with two jets.
- $W^\pm \rightarrow \ell^\pm \nu_\ell$ and $V (W^\pm/Z) \rightarrow q\bar{q}$.
- The signature consists of 4 jets, 1 lepton and missing E_T .

Event Selection:

- Two categories:
 - Resolved: Four anti- k_T jets with distance parameter $\Delta R = 0.4$ (AK4)
 - Boosted: Two anti- k_T jets with $\Delta R = 0.4$ and one jet with $\Delta R = 0.8$ (AK8).
- $m_{jj}^{VBS} > 500$ GeV and $\Delta\eta_{jj}^{VBS} > 2.5$ for tag jets (enhances VBS events)
- No b-jets should be found in the signal region

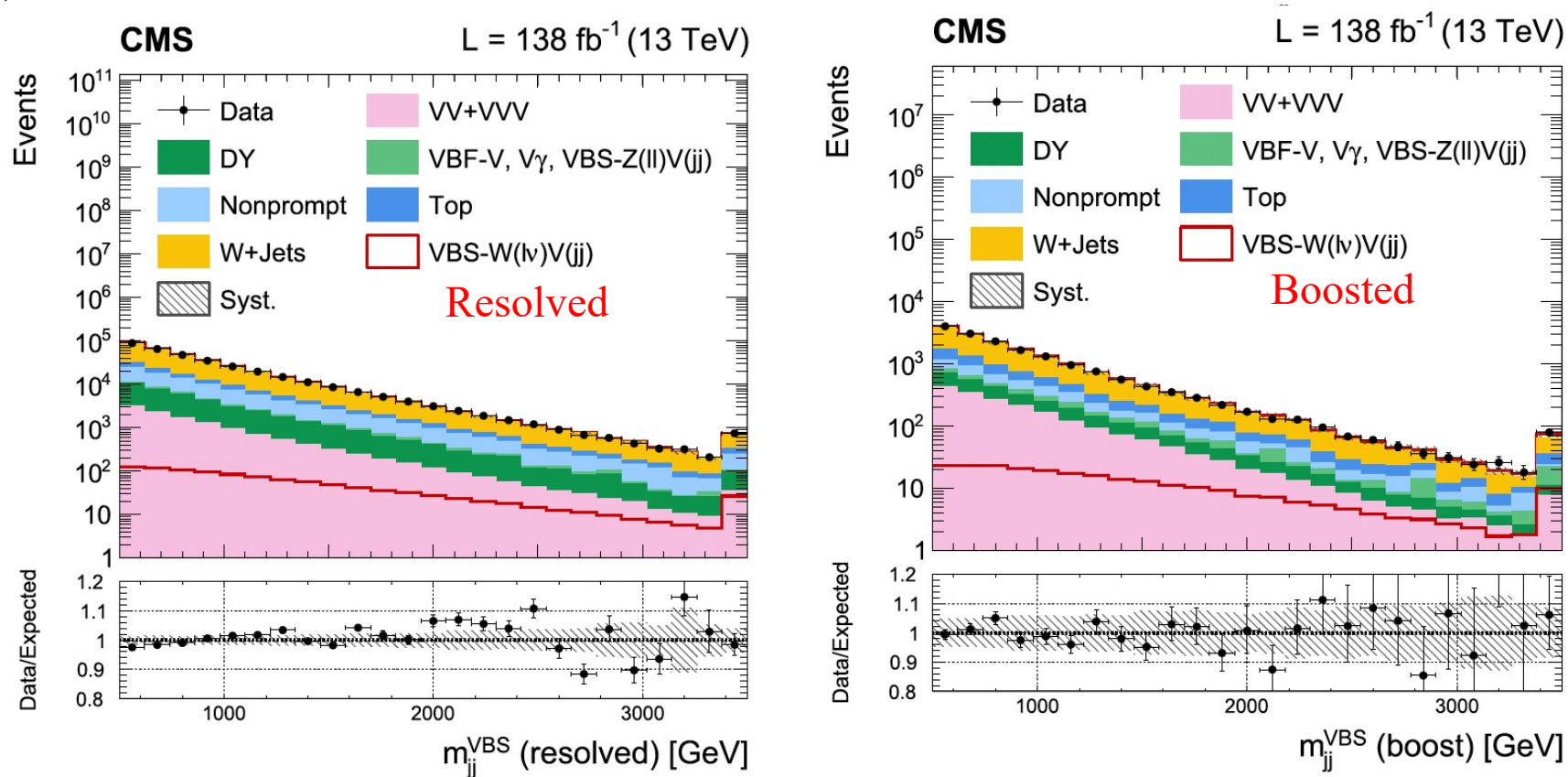


Backgrounds:

- $W + jets$ (data-driven method) using dedicated CRs.
- Top quark background, QCD-multijet
- VBF-V Single vector boson EW production (2% in resolved, 4% in boosted)
- Other: QCD VBS WV production, Drell-Yan, VVV, $V\gamma$, VBS $Z(\ell\ell)V(jj)$

WVjj: Cross-section Measurements

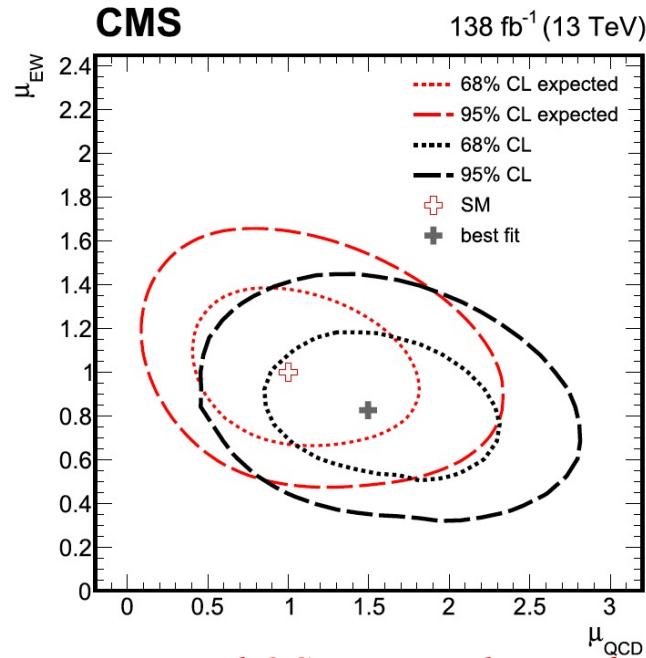
- Deep Neural Network (DNN) used for signal extraction.
- It increases the sensitivity of the analysis by a factor of 3 over a fit to the shape of the m_{jj}^{VBS} variable (most sensitive variable).



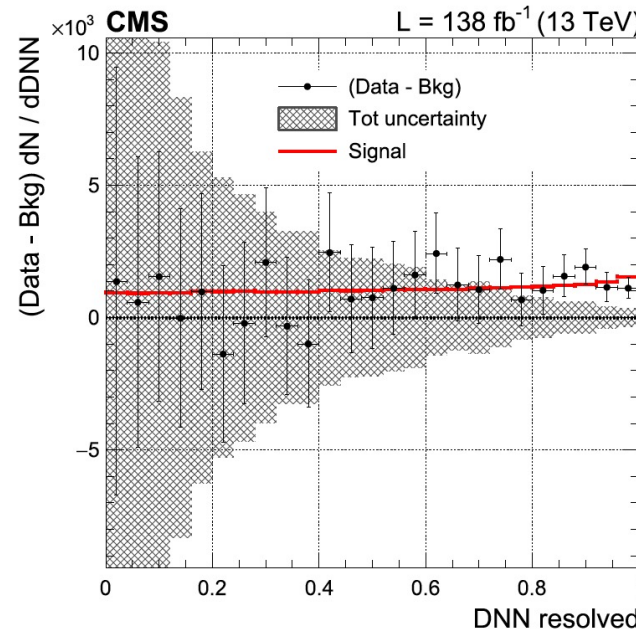
Post-fit distributions of m_{jj}^{VBS} in the resolved and boosted categories.

WVjj: Cross-section Measurements

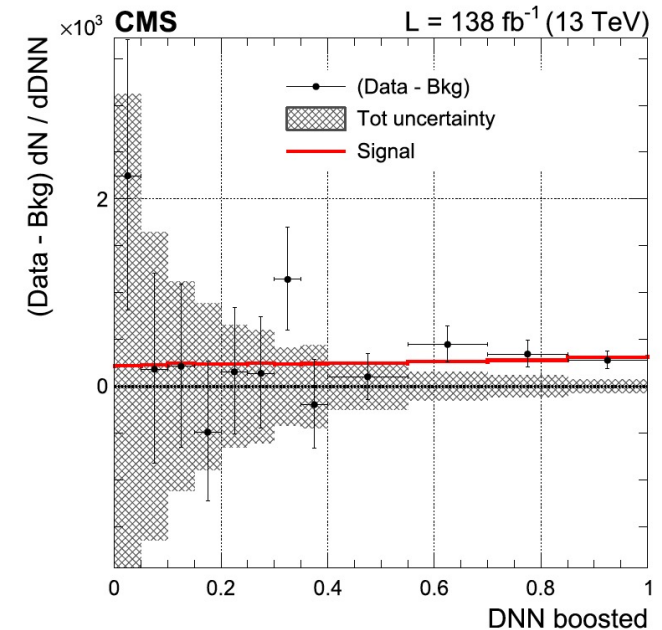
- The cross-section measured at a fiducial phase space defined at parton level.
- Cross-section measurement:
 - Measured: $1.90^{+0.53}_{-0.46} pb$
 - Expected: $2.23^{+0.08}_{-0.11} (scale) \pm 0.05 (PDF) pb$
- Observed EW signal strength: $\mu_{EW} = 0.85 \pm 0.12 (stat)_{-0.17}^{+0.19} (syst)$ with an obs (exp) significance of 4.4σ (5.1σ), with QCD associated diboson production fixed to SM prediction.
- EW + QCD associated signal strength: $0.97 \pm 0.06 (stat)_{-0.21}^{+0.19} (syst)$.



Simultaneous EW and QCD WV production fit: Exp and Obs 68% and 95% CL contours for signal strengths



DNN Score Distribution



ZZ + jets: Differential Cross-section Measurement

- Differential production cross-section of ZZ + jets as a function of multiple variables.
- Signal includes $qq \rightarrow ZZ$ sample, $gg \rightarrow ZZ$ samples, EW production sample (which includes vector boson fusion (VBF) Higgs events and their interference with non-Higgs EW production), and the $gg \rightarrow H \rightarrow ZZ$ samples

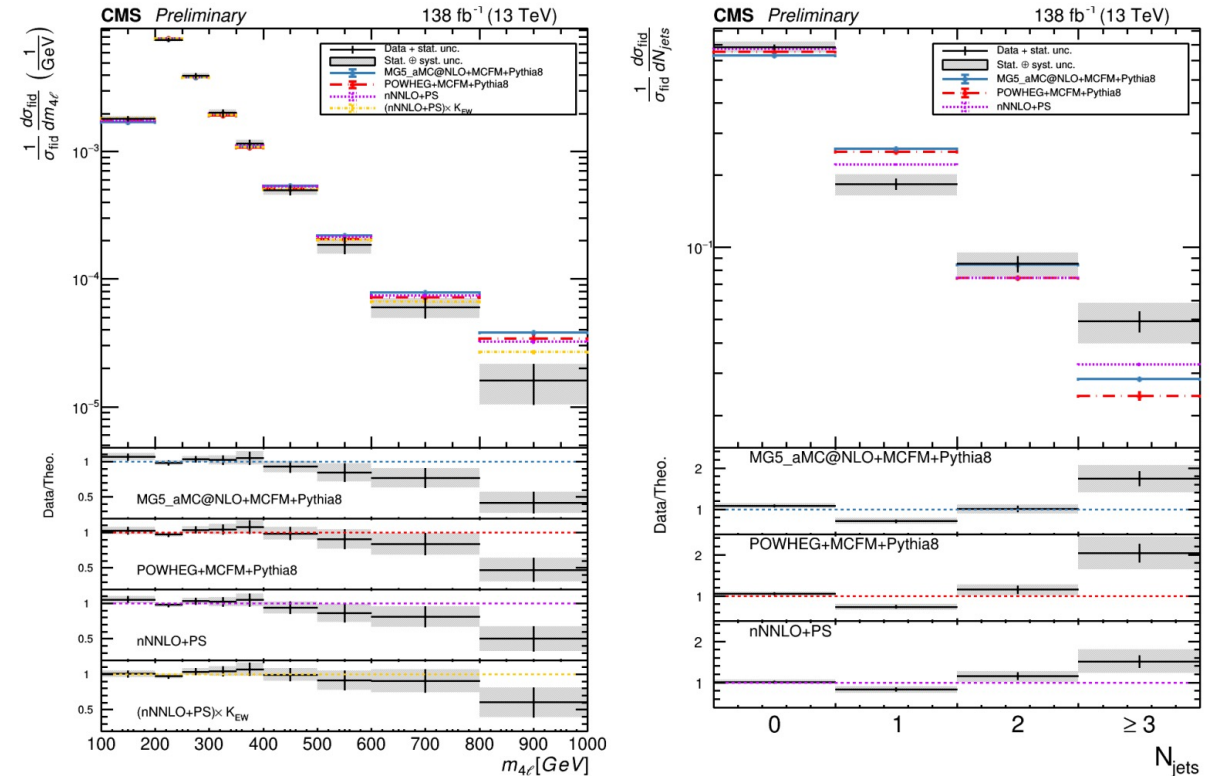
Event Selection:

- Fully leptonic final states. Lepton-lepton and jet-lepton (or photon) overlaps are taken care of. Four-lepton candidates of SFOC pairs are considered.
- Jets with $p_T > 30$ GeV and $|\eta| < 4.7$.

Backgrounds:

- Well reconstructed and isolated lepton candidates suppress backgrounds to a great extent
- Backgrounds dominated by $Z + jets$, $WZ + jets$, $t\bar{t}$, VVV .

8/30/23



Differential cross-section for $m_{4\ell}$ and N_{jets} .

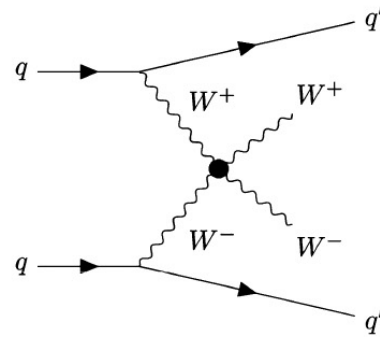
- Unfolding using the iterative D'Agostini's method
- EW corrections improves the description of the $m_{4\ell}$ distribution.

- Electroweak production of W^+W^- associated with two jets.

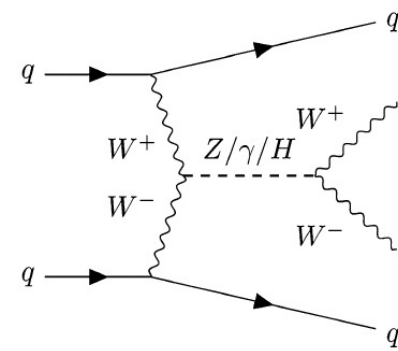
Event Selection:

- Fully leptonic final states. Split into different flavor SRs: e^+e^- , $\mu^+\mu^-$, $e^\pm\mu^\mp$.
 - exactly two opposite-sign leptons (electrons or muons) $m_{\ell\ell} > 50$ GeV and $p_T^{\ell\ell} > 30$ GeV
 - two jets with large pseudorapidity separation and high dijet invariant mass: $m_{jj} > 300$ GeV and $|\Delta\eta_{jj}| > 2.5$
 - $p_T^{miss} > 20$ GeV
 - SR split acc to the final state lepton flavors, Zeppenfeld variable: $Z_{\ell\ell} = \frac{1}{2}|Z_{\ell 1} + Z_{\ell 2}|$, where $Z_\ell = \eta_\ell - \frac{1}{2}(\eta_{j_1} + \eta_{j_2})$.

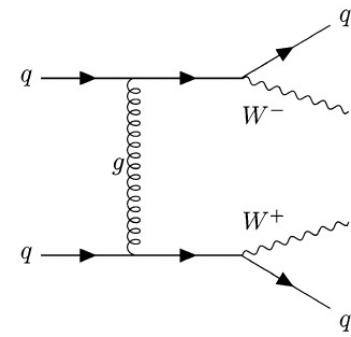
EW production



EW production



QCD Induced production



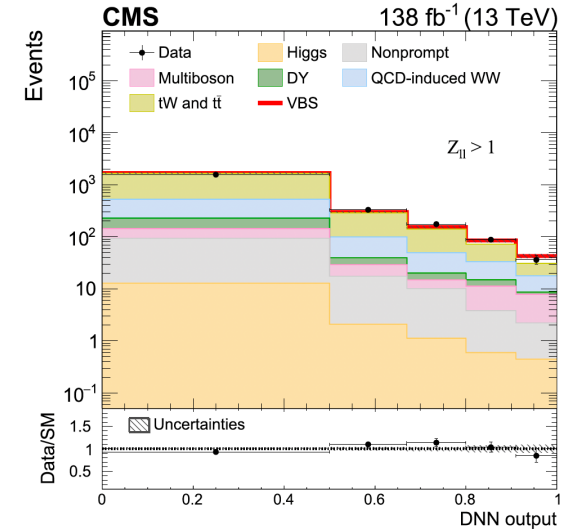
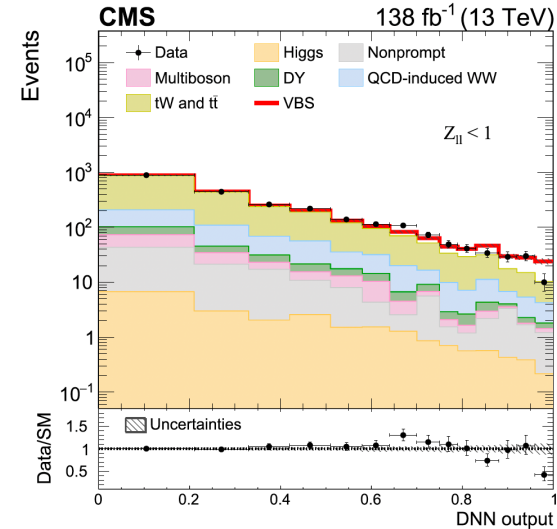
Backgrounds:

- $t\bar{t}$: estimated with a $t\bar{t}$ CR
- Drell-Yan production: estimated with dedicated CRs
- QCD induced W^+W^- : Normalization is left floating in the fit
- Non-prompt leptons: $W + jets$ - From data, $Z + jets$ - From simulation
- Higgs and multiboson production: using simulation

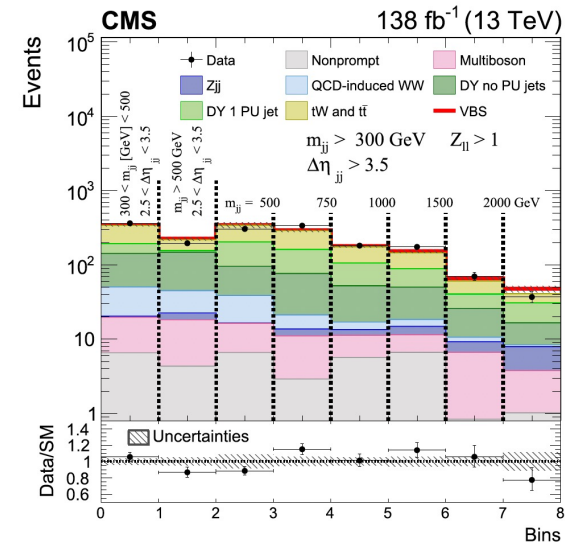
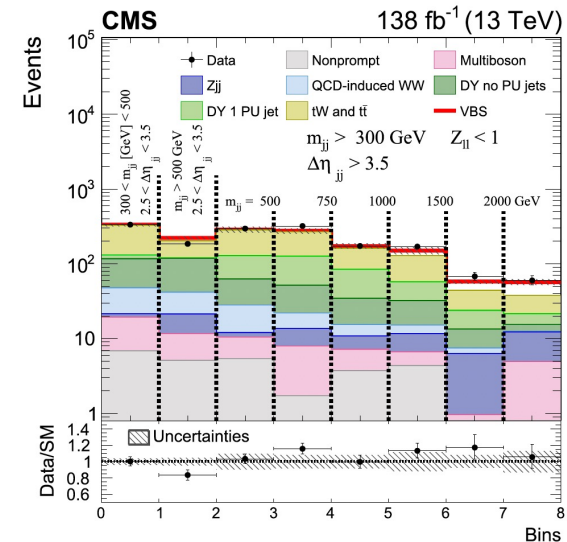
(Opposite Sign) EW W^+W^-jj Measurement

PLB 841 (2023) 137495

- In the $e\mu$ category, a feed forward deep neural network (DNN) is used to distinguish signal from $t\bar{t}$ and QCD induced W^+W^- .
- Separate models built for $Z_{\ell\ell} < 1$ (less background, signal enriched) and $Z_{\ell\ell} > 1$.
- Binary cross-entropy loss function is minimized in both the models
- $\mu_{EW} = \sigma^{obs} / \sigma^{SM}$ is the parameter of interest. Translated to cross-section in two fiducial volumes.
- A maximum-likelihood fit is performed to get the cross-sections:
- The background only hypothesis (without contribution from EW W^+W^-) rejected with obs (exp) significance of 5.6σ (5.2σ).
 - More inclusive region: $99 \pm 20 fb$ (LO prediction of $89 \pm 5 (scale)fb$)
 - Closer to the preselection region: $10.2 \pm 2.0 fb$ (LO theoretical prediction is $9.1 \pm 0.6 (scale)fb$)



DNN Output Distribution in Diff Flavor ($e\mu$) Channel



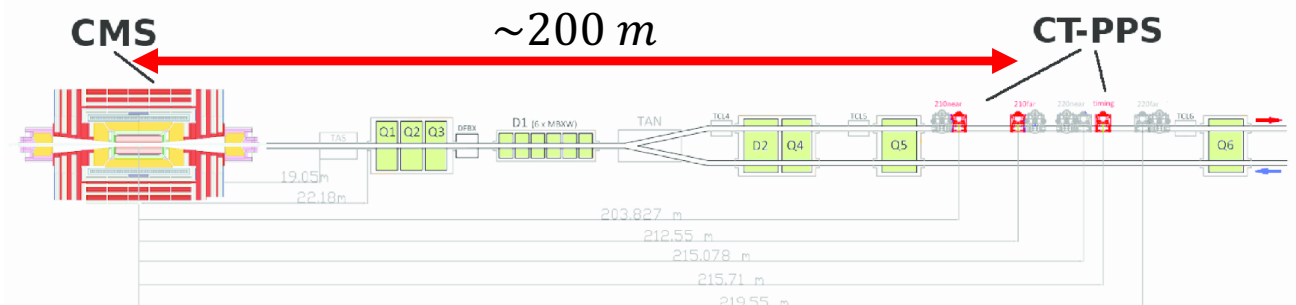
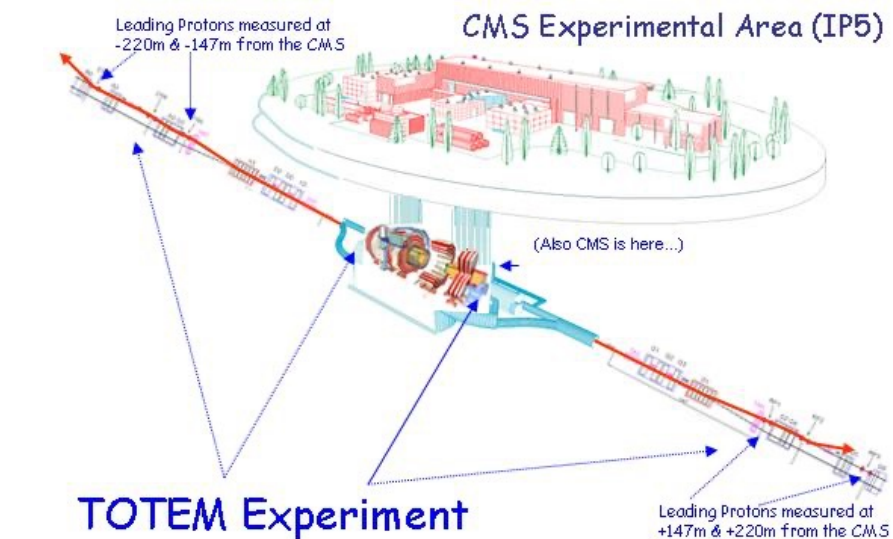
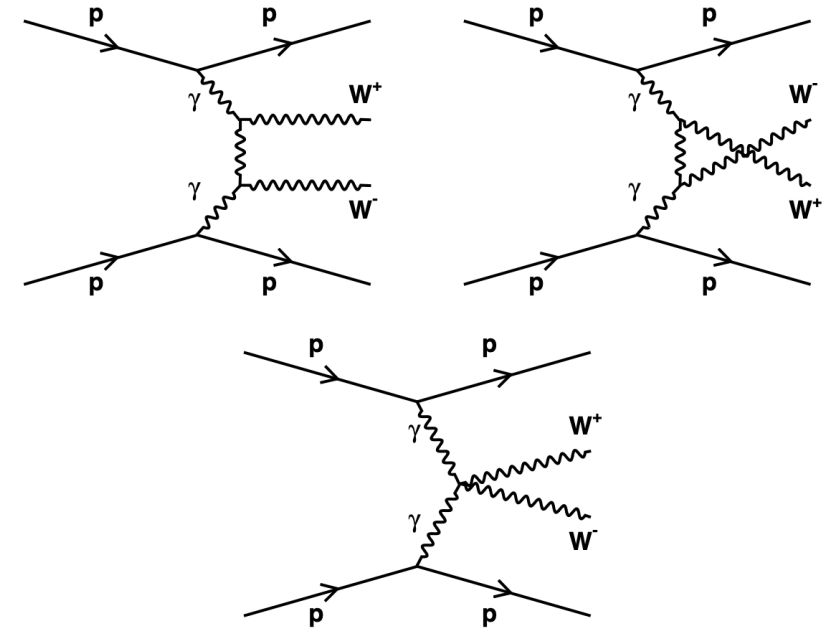
Regions in m_{jj} and $|\Delta\eta_{jj}|$ same Flavor (ee and $\mu\mu$)

5

$\gamma\gamma \rightarrow WW$ and $\gamma\gamma \rightarrow ZZ$ CMS+TOTEM

[arXiv:2211.16320v2](https://arxiv.org/abs/2211.16320v2)

- Search for exclusive high mass $\gamma\gamma \rightarrow WW$ and $\gamma\gamma \rightarrow ZZ$ production in pp collisions with an integrated luminosity of 100 fb^{-1} .
- Using intact forward protons reconstructed in near-beam detectors
- Both weak bosons decaying into boosted and merged jets
- The protons radiate quasireal high-energy photons and remain intact. Only the two photons interact, and the protons are scattered at very small angles.
- The scattered protons are measured using a Precision Proton Spectrometer (PPS) of CMS-TOTEM collaboration.



$\gamma\gamma \rightarrow WW$ and $\gamma\gamma \rightarrow ZZ$: EFT interpretations

Event Reco and selection:

- The scattered protons are reconstructed using “Multi-RP Algorithm”. which combines tracks reconstructed in both tracking Roman pots in each arm of PPS.
- Both weak bosons decaying into boosted and merged jets.
- Proton jet matching is performed, and signal regions are defined using variables $1 - m(VV)/m(pp)$ and $y(pp) - y(VV)$.

Coupling	Observed (expected) 95% CL upper limit No clipping	Observed (expected) 95% CL upper limit Clipping at 1.4 TeV
$ a_0^W / \Lambda^2 $	4.3 (3.9) $\times 10^{-6} \text{ GeV}^{-2}$	5.2 (5.1) $\times 10^{-6} \text{ GeV}^{-2}$
$ a_C^W / \Lambda^2 $	1.6 (1.4) $\times 10^{-5} \text{ GeV}^{-2}$	2.0 (2.0) $\times 10^{-5} \text{ GeV}^{-2}$
$ a_0^Z / \Lambda^2 $	0.9 (1.0) $\times 10^{-5} \text{ GeV}^{-2}$	—
$ a_C^Z / \Lambda^2 $	4.0 (4.5) $\times 10^{-5} \text{ GeV}^{-2}$	—

*Expected and observed limits on dimension-6
AQGC operators*

Backgrounds:

- QCD multijet, $W + jets$, $Z + jets$, $t\bar{t}$. Have to rely on data for background estimate as the protons predominantly arise from diffractive pileup interactions, which are not well modelled.

$\gamma\gamma \rightarrow WW$ and $\gamma\gamma \rightarrow ZZ$: EFT interpretations

- Translation to linear dimension-8 mixed AQGCs (contain both covariant derivatives of the Higgs field and field strength tensor) in case of processes involving photons:

$$a_0^W = -\frac{m_W}{\pi\alpha_{\text{em}}} \left[s_w^2 \frac{f_{M,0}}{\Lambda^2} + 2c_w^2 \frac{f_{M,2}}{\Lambda^2} + s_w c_w \frac{f_{M,4}}{\Lambda^2} \right].$$

- The limits are obtained for a fiducial region of $0.04 < \xi < 0.20$ and diboson invariant mass $m(VV) > 1$ TeV, and correspond to the diboson production cross section before decays into hadrons (p_{nom} nominal beam momentum, p scattered proton momentum).

$$\xi = (p_{\text{nom}} - p) / p_{\text{nom}}.$$

- Upper exclusion limits on AQGC like signal at 95% CL obs (exp):

- $\sigma(pp \rightarrow pWWp) < 67(53_{-19}^{+34}) fb$
- $\sigma(pp \rightarrow pZZp) < 43(62_{-20}^{+33}) fb$.

Coupling	Observed (expected) 95% CL upper limit No clipping	Observed (expected) 95% CL upper limit Clipping at 1.4 TeV
$ f_{M,0}/\Lambda^4 $	66.0 (60.0) TeV ⁻⁴	79.8 (78.2) TeV ⁻⁴
$ f_{M,1}/\Lambda^4 $	245.5 (214.8) TeV ⁻⁴	306.8 (306.8) TeV ⁻⁴
$ f_{M,2}/\Lambda^4 $	9.8 (9.0) TeV ⁻⁴	11.9 (11.8) TeV ⁻⁴
$ f_{M,3}/\Lambda^4 $	73.0 (64.6) TeV ⁻⁴	91.3 (92.3) TeV ⁻⁴
$ f_{M,4}/\Lambda^4 $	36.0 (32.9) TeV ⁻⁴	43.5 (42.9) TeV ⁻⁴
$ f_{M,5}/\Lambda^4 $	67.0 (58.9) TeV ⁻⁴	83.7 (84.1) TeV ⁻⁴
$ f_{M,7}/\Lambda^4 $	490.9 (429.6) TeV ⁻⁴	613.7 (613.7) TeV ⁻⁴

Conversion of limits to dim-8 operators with assumption that all $f_{M,i}$ except one are equal to zero.

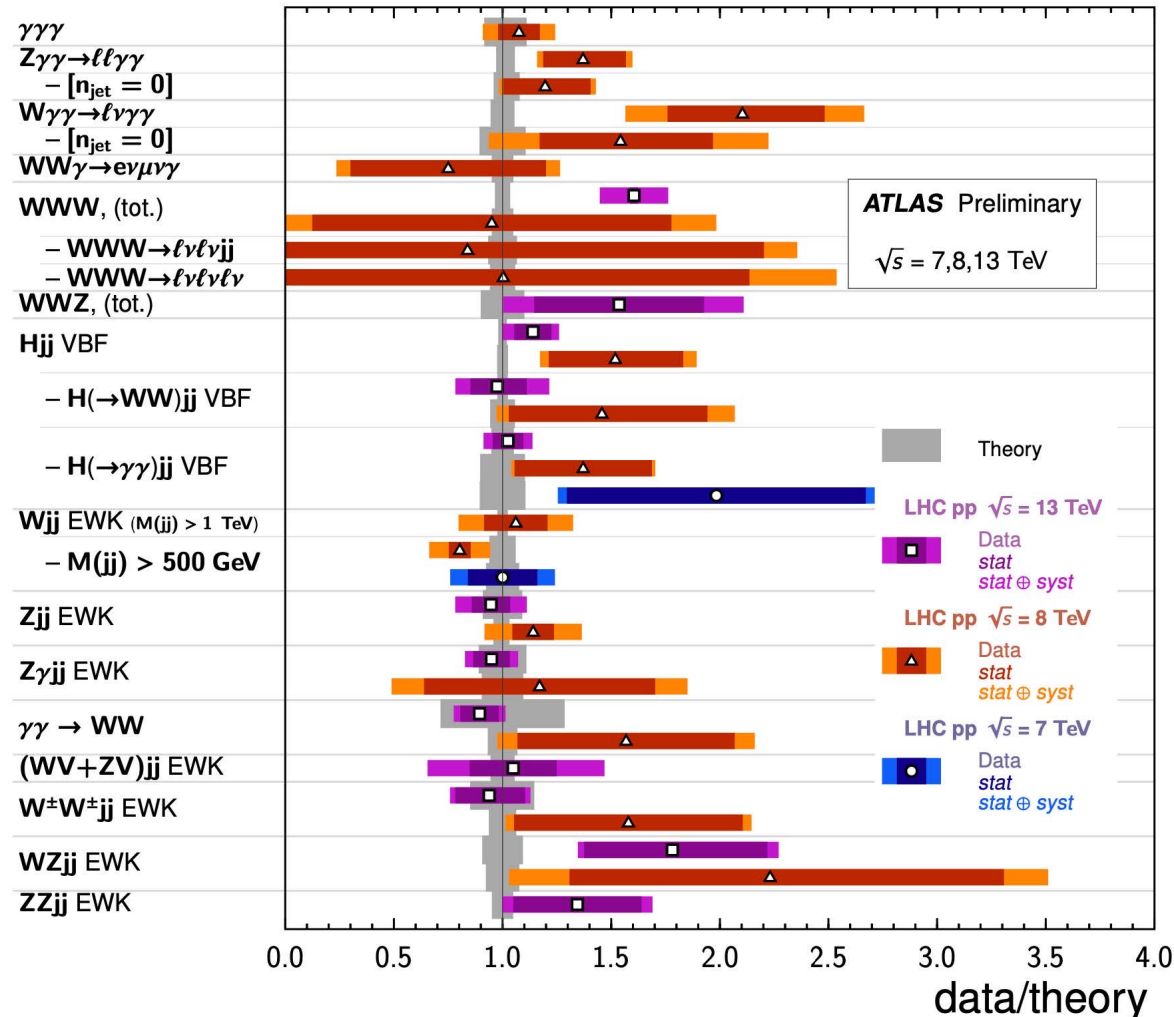
Summary

- Overview (not exhaustive) of the latest massive diboson final state analyses from 2022 and 2023 performed at the ATLAS and CMS collaborations.
- Many jet associated diboson processes are observed with a more than 5σ with respect to the background only hypothesis.
- More precise limits on anomalous couplings with EFT interpretations (dim-6 and dim-8 operators) in many different channels are performed.
- First diboson longitudinal-longitudinal measurements performed for WZ and ZZ, with first observation of WZ longitudinal-longitudinal in ATLAS.
- Other BSM searches, study of CP properties, etc are also performed.
- Many more analyses coming soon with polarization measurements, EFT interpretations and BSM searches in the massive diboson channels.

Backup

Previous Multiboson Searches in Run 2: ATLAS

VBF, VBS, and Triboson Cross Section Measurements Status: February 2022



- This talk includes latest results for:
- $ZZjj$: Differential Cross-section and EFT Interpretations
 - Measurement of Longitudinal-longitudinal ZZ (Z_L, Z_L) and Study of CP Property
 - (Same sign) $W^\pm W^\pm jj$:
 - (Opposite Sign) $W^+ W^-$
 - (Opposite Sign) $W^+ W^- jj$
 - $W^\pm Z$ Joint Polarization Measurements

EFT Interpretations: Dimension-six op

Wilson coefficient	$ \mathcal{M}_{d6} ^2$ Included	95% confidence interval [TeV ⁻²]	
		Expected	Observed
c_W/Λ^2	yes	[-1.3, 1.3]	[-1.2, 1.2]
	no	[-32, 32]	[-37, 28]
$c_{\widetilde{W}}/\Lambda^2$	yes	[-1.3, 1.3]	[-1.2, 1.2]
	no	[-17, 17]*	[0, 30]*
c_{HWB}/Λ^2	yes	[-16, 7]	[-16, 6]
	no	[-12, 12]	[-15, 10]
$c_{H\widetilde{W}B}/\Lambda^2$	yes	[-1.3, 1.3]	[-1.2, 1.2]
	no	[-67, 67]*	[-25, 130]*
c_{HB}/Λ^2	yes	[-13, 13]	[-12, 12]
	no	[-38, 38]	[-38, 38]
$c_{H\widetilde{B}}/\Lambda^2$	yes	[-13, 13]	[-12, 12]
	no	[-420, 420]*	[-200, 790]*

(Same sign) $W^\pm W^\pm jj$ ATLAS

Event Selection:

- Expected purity of the EW, QCD and interference is 52%, 5.4% and 1.7%.

Exactly two signal leptons with $p_T > 27$ GeV and the same electric charge with $|\eta| < 2.5$ for muons and with $|\eta| < 2.47$ excluding $1.37 \leq |\eta| \leq 1.52$ for electrons with $|\eta| < 1.37$ in the ee channel

$m_{\ell\ell'} \geq 20$ GeV

3rd lepton veto

$|m_{ee} - m_Z| > 15$ GeV in the ee -channel

$E_T^{\text{miss}} \geq 30$ GeV

At least two jets

Leading and subleading jets satisfying $p_T > 65$ GeV and $p_T > 35$ GeV, respectively

b -jet veto for jets with $p_T > 20$ GeV and $|\eta| < 2.5$

$m_{jj} \geq 500$ GeV

$|\Delta y_{jj}| > 2$

Backgrounds:

- WZ/γ^* (22% of the signal event yield): One lepton escaping the third lepton veto requirement.
- Non-Prompt Lepton Background (12% of the signal event yield): W +jets, semi-leptonic $t\bar{t}$. Estimated using data-driven method
- Electron charge misidentification background: From Z and dileptonic $t\bar{t}$.
- Other backgrounds: $V\gamma$ (2.4%), ZZ , $t\bar{t}V$, VVV (except same sign WW) (total 1.6%)

Same sign WWjj uncertainties

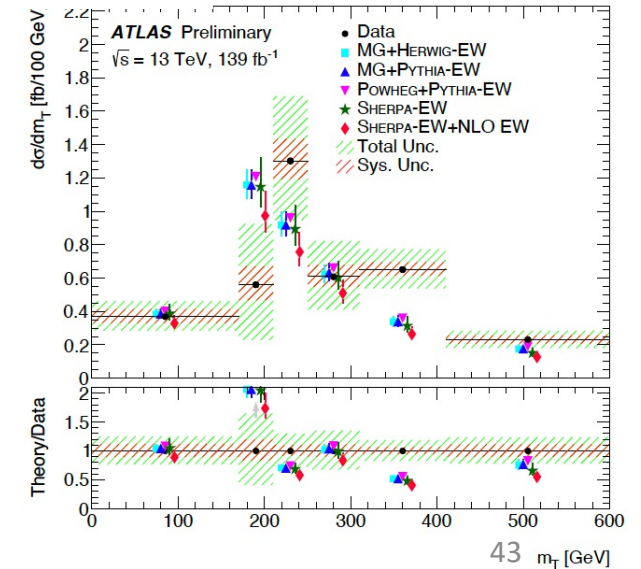
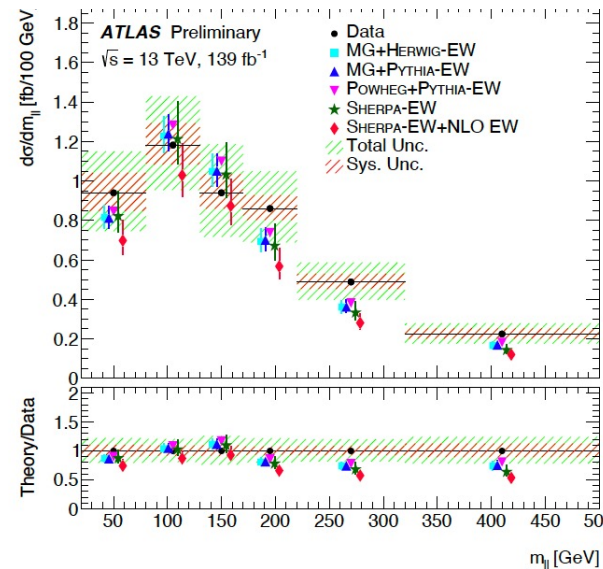
Source	Impact [%]
Experimental	
Electron calibration	0.4
Muon calibration	0.5
Jet energy scale and resolution	1.8
E_T^{miss} scale and resolution	0.2
b -tagging inefficiency	0.7
Background, misid. leptons	3.1
Background, charge misrec.	0.8
Pileup modelling	0.2
Luminosity	1.9
Modelling	
EW $W^\pm W^\pm jj$, shower, scale, PDF & α_s	0.8
EW $W^\pm W^\pm jj$, QCD corrections	3.5
EW $W^\pm W^\pm jj$, EW corrections	0.8
Int $W^\pm W^\pm jj$, shower, scale, PDF & α_s	0.1
QCD $W^\pm W^\pm jj$, shower, scale, PDF & α_s	2.3
QCD $W^\pm W^\pm jj$, QCD corrections	0.9
Background, WZ scale, PDF & α_s	0.2
Background, WZ reweighting	1.7
Background, other	1.0
Model statistical	1.8
Experimental and modelling	6.7
Data statistical	7.4
Total	10.0

(Same sign) $W^\pm W^\pm jj$ ATLAS

- Fiducial Cross-section measurement: Fiducial region defined as close to analysis signal region and detector acceptance as possible.
 - Signal region split in 4 regions according to the lepton flavors in the final state

Description	$\sigma_{\text{fid}}^{\text{EW}}$, fb	$\sigma_{\text{fid}}^{\text{EW+Int+QCD}}$, fb
Measured cross section	2.88 ± 0.21 (stat.) ± 0.19 (syst.)	3.35 ± 0.22 (stat.) ± 0.20 (syst.)
MG_AMC@NLO+HERWIG	2.53 ± 0.04 (PDF) $\pm_{0.19}^{0.22}$ (scale)	2.93 ± 0.05 (PDF) $\pm_{0.27}^{0.34}$ (scale)
MG_AMC@NLO+PYTHIA	2.55 ± 0.04 (PDF) $\pm_{0.19}^{0.22}$ (scale)	2.94 ± 0.05 (PDF) $\pm_{0.27}^{0.33}$ (scale)
SHERPA	2.44 ± 0.03 (PDF) $\pm_{0.27}^{0.40}$ (scale)	2.80 ± 0.03 (PDF) $\pm_{0.36}^{0.53}$ (scale)
POWHEG BOX +PYTHIA	2.67	—

- Differential cross-section measurement. Likelihood based unfolding used to get particle level distributions
- Good agreement between data/MC within uncertainties. χ^2 and p-value measured to check data-MC compatibility. P-values range from 0.014 to 0.623 across five variables used: $m_{\ell\ell}$, m_{jj} , m_T , $N_{\text{gap jets}}$ (num of jets between two signal jets in rapidity) and Zeppenfeld variable.

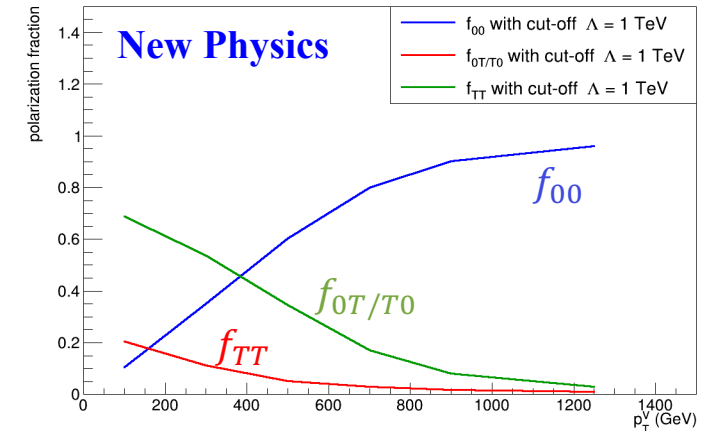


$W^\pm Z$ Polarization Studies in ATLAS

[arXiv:2211.09435](https://arxiv.org/abs/2211.09435)

- Motivation:**

- Goldstone Boson Equivalence Theorem: a phenomenon at high energies ([PRD 103 \(2021\) 053007](#))
- The V_0V_0 (both longitudinally polarized bosons) are the only polarization states that exhibit quadratic energy growth for BSM amplitudes, thus giving us a handle to search for new physics. ([JHEP 02 \(2018\) 111](#))

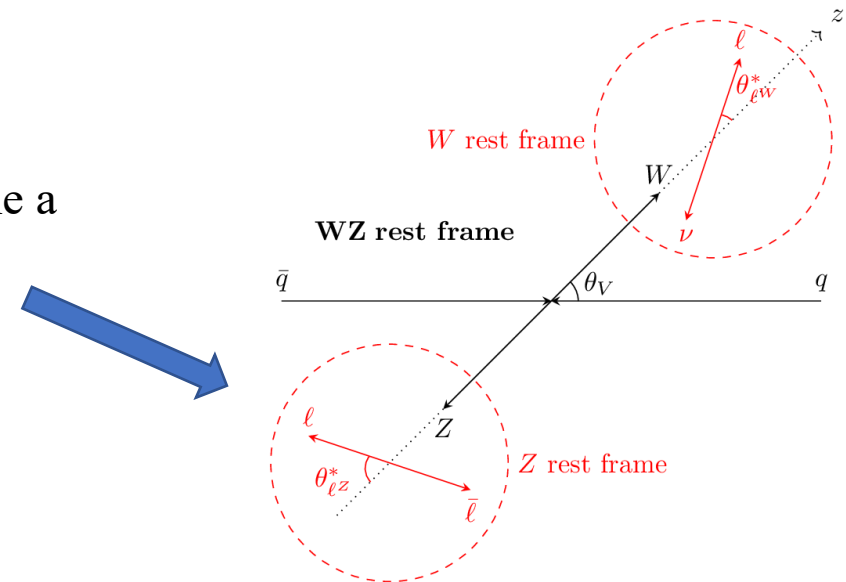


Polarization fractions as a function of p_T^V for a new physics model with a cut off $\Lambda = 1$ TeV using calculations from [PRD 99 \(2019\) 055001](#)

- **This is the first-ever observation of longitudinal-longitudinal joint polarization state in diboson production.**

- **Some of the challenges:**

- The definition of polarization is not Lorentz invariant, so must define a frame – modified helicity frame
- Should discriminate both bosons at once. Combining L and R polarization there are 4 configurations to distinguish (W_0Z_0 , W_0Z_T , W_TZ_0 , W_TZ_T , where 0 is longitudinal and T is transverse)



Previous Multiboson Searches in Run 2: CMS

Electroweak

W	7 TeV	JHEP 10 (2011) 132
W	8 TeV	PRL 112 (2014) 191802
W	13 TeV	SMP-15-004
Z	7 TeV	JHEP 10 (2011) 132
Z	8 TeV	PRL 112 (2014) 191802
Z	13 TeV	SMP-15-011

di-Boson

Wy	7 TeV	PRD 89 (2014) 092005
Wy	13 TeV	PRL 126 252002 (2021)
Zy	7 TeV	PRD 89 (2014) 092005
Zy	8 TeV	JHEP 04 (2015) 164
WW	7 TeV	EPJC 73 (2013) 2610
WW	8 TeV	EPJC 76 (2016) 401
WW	13 TeV	PRD 102 092001 (2020)
WZ	7 TeV	EPJC 77 (2017) 236
WZ	8 TeV	EPJC 77 (2017) 236
WZ	13 TeV	JHEP 07 (2022) 032
ZZ	7 TeV	JHEP 01 (2013) 063
ZZ	8 TeV	PLB 740 (2015) 250
ZZ	13 TeV	EPJC 81 (2021) 200

tri-Boson

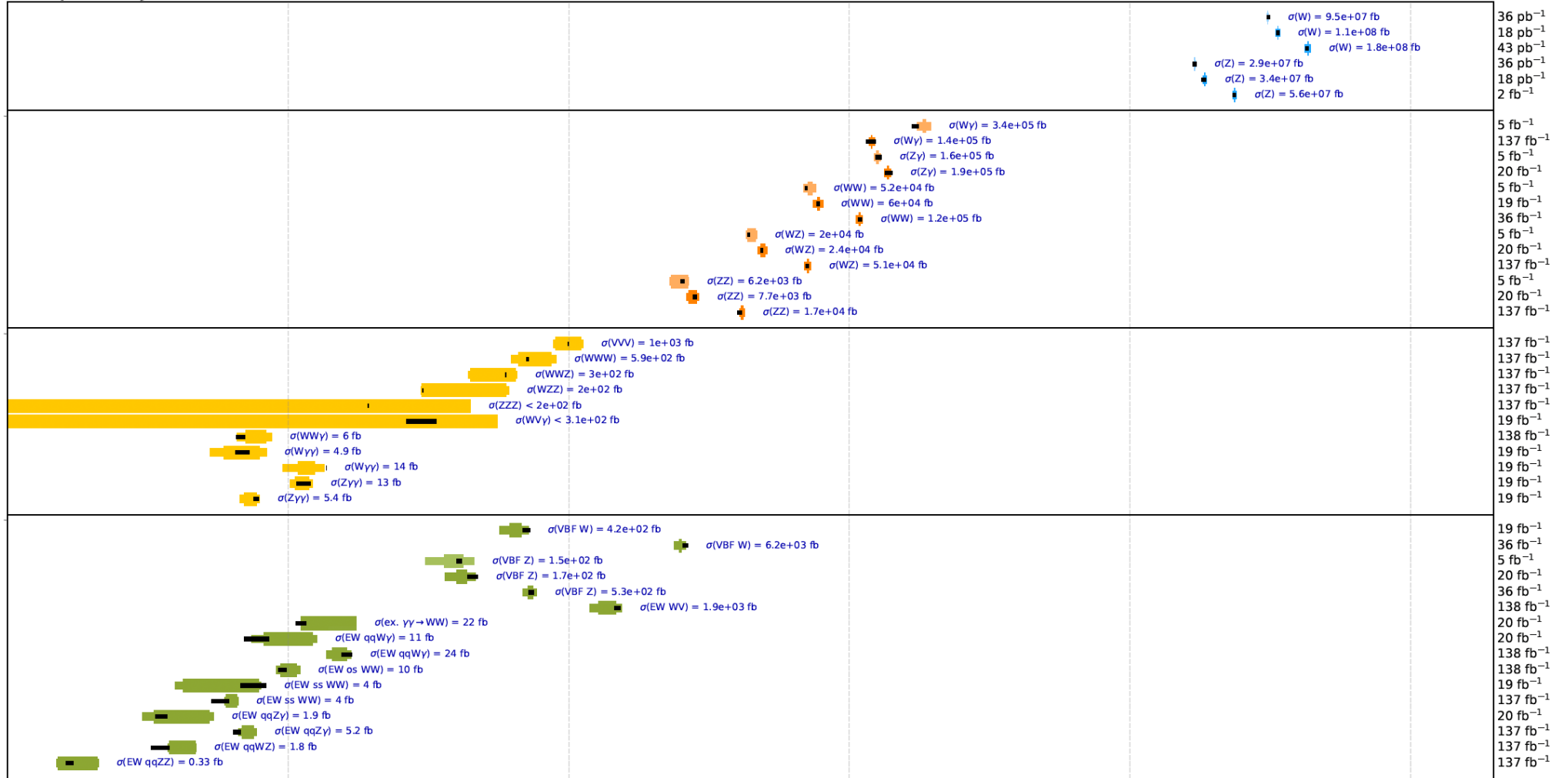
VVV	13 TeV	PRL 125 151802 (2020)
WWW	13 TeV	PRL 125 151802 (2020)
WWZ	13 TeV	PRL 125 151802 (2020)
WZZ	13 TeV	PRL 125 151802 (2020)
ZZZ	13 TeV	PRL 125 151802 (2020)
WWγ	8 TeV	PRD 90 032008 (2014)
WWγ	13 TeV	SMP-22-006
Wγγ	8 TeV	JHEP 10 (2017) 072
Wγγ	13 TeV	JHEP 10 (2021) 174
Zγγ	8 TeV	JHEP 10 (2017) 072
Zγγ	13 TeV	JHEP 10 (2021) 174

VBF and VBS

VBF W	8 TeV	JHEP 11 (2016) 147
VBF W	13 TeV	EPJC 80 (2020) 43
VBF Z	7 TeV	JHEP 10 (2013) 101
VBF Z	8 TeV	EPJC 75 (2015) 66
VBF Z	13 TeV	EPJC 78 (2018) 589
EW WW	13 TeV	PLB 834 (2022) 137438
ex. γγ → WW	8 TeV	JHEP 08 (2016) 119
EW qqWγ	8 TeV	JHEP 06 (2017) 106
EW qqWγ	13 TeV	Accepted by PRD
EW os WW	13 TeV	Submitted to PLB
EW ss WW	8 TeV	PRL 114 051801 (2015)
EW ss WW	13 TeV	PRL 120 081801 (2018)
EW qqZγ	8 TeV	PLB 770 (2017) 380
EW qqZγ	13 TeV	PRD 104 072001 (2021)
EW qqWZ	13 TeV	PLB 809 (2020) 135710
EW qqZZ	13 TeV	PLB 812 (2020) 135992

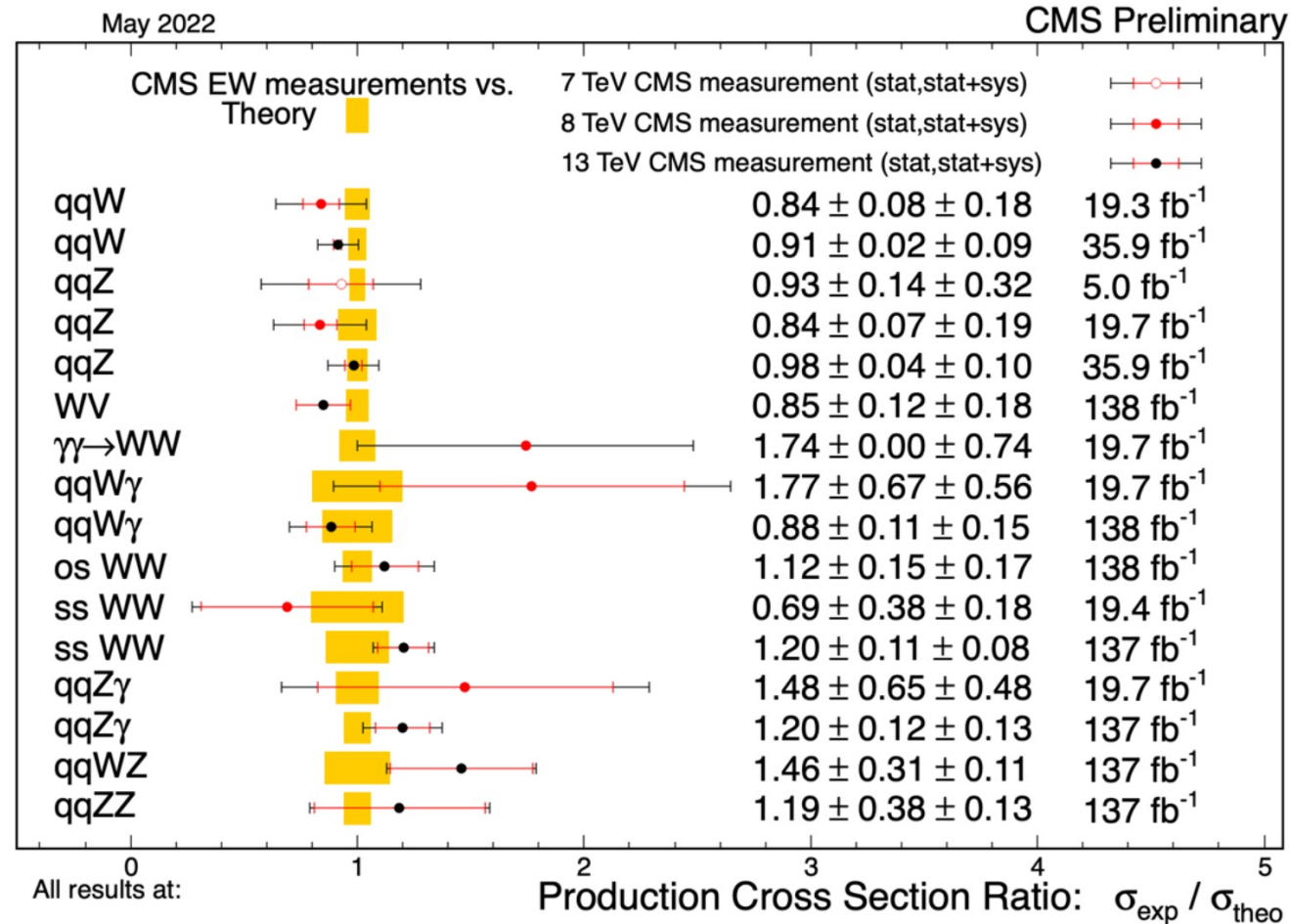
CMS preliminary

18 pb⁻¹ - 138 fb⁻¹ (7,8,13,13.6 TeV)

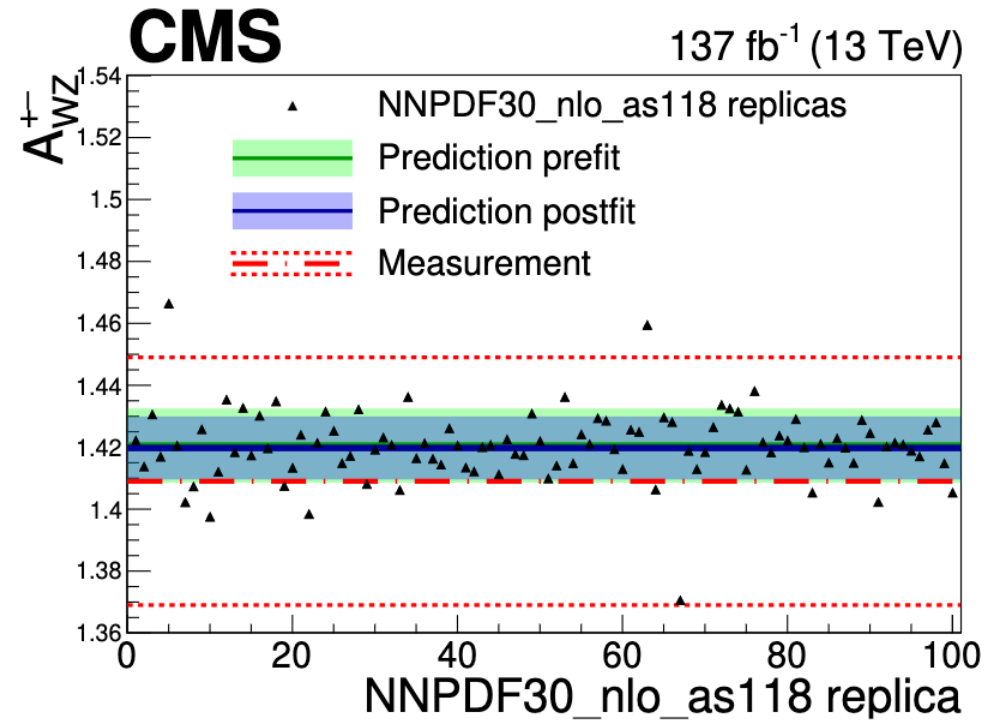
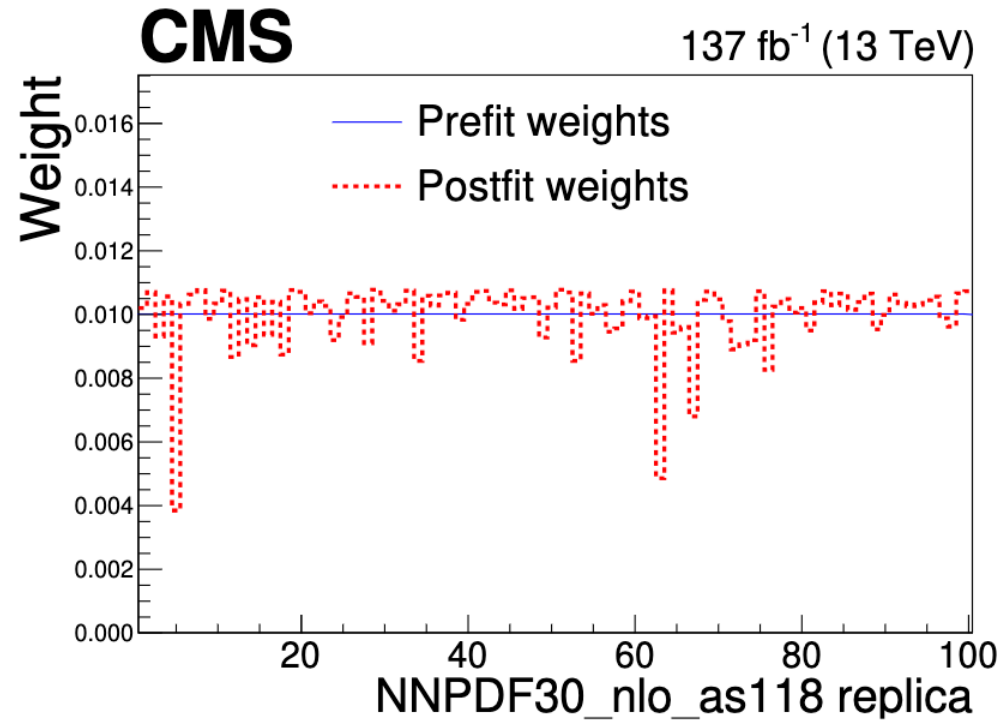


X-axis: $\sigma(fb)$

Previous Multiboson Searches in Run 2: CMS

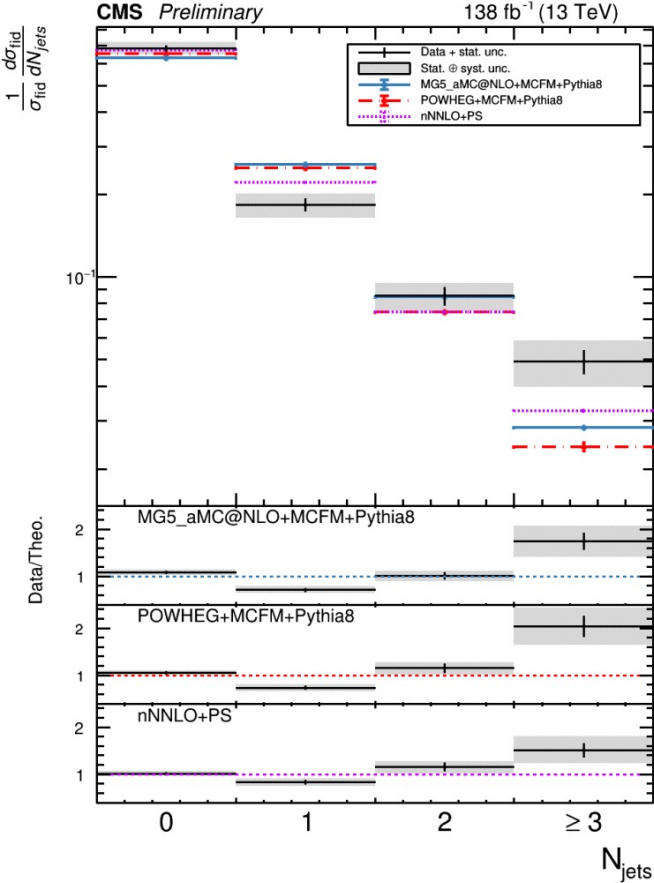
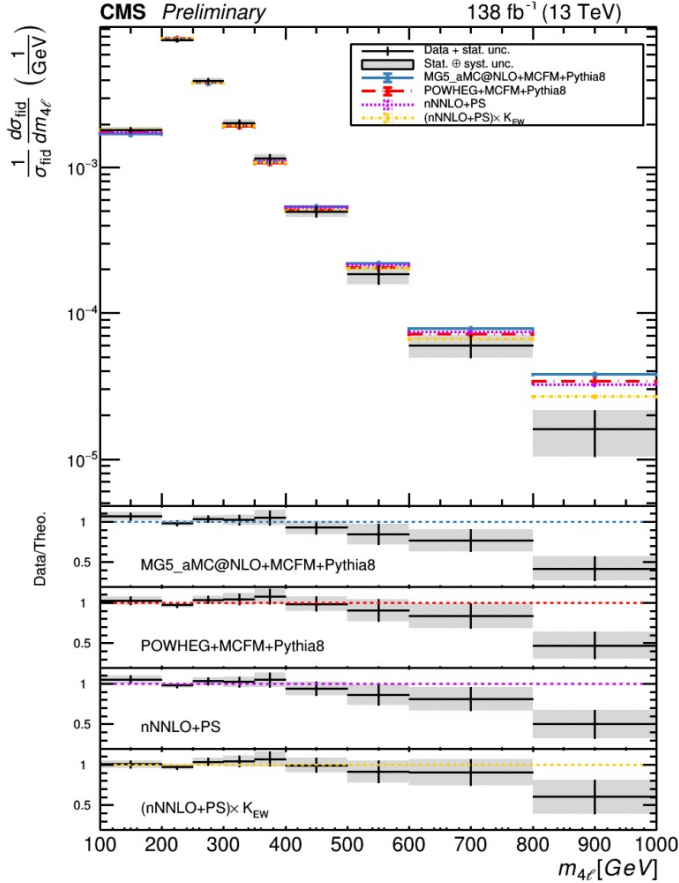


WZ CMS



ZZ + jets CMS

- Unfolding using the iterative D’Agostini’s method including correction for background contributions.
- Differential cross-section measured for: number of jets, jets transverse momentum and pseudorapidity, invariant mass of dijet system and pseudorapidity difference of the highest-pT and second-highest-pT jets, invariant mass of the four leptons with different jet multiplicities in the events
- The nNNLO+PS prediction describes the distribution of jet multiplicities better than MadGraph5 aMC@NLO and POWHEG
- the inclusion of EW corrections improves the description of the $m_{4\ell}$ distribution.
- Further improvement of the predictions is required to describe the ZZ+jet production in the whole phase space.



Zjj CMS: EFT Limits

$$\begin{aligned} -0.24 < f_{T0} / \Lambda^4 < 0.22 \\ -0.31 < f_{T1} / \Lambda^4 < 0.31 \\ -0.63 < f_{T2} / \Lambda^4 < 0.59 \\ -0.43 < f_{T8} / \Lambda^4 < 0.43 \\ -0.92 < f_{T9} / \Lambda^4 < 0.92 \end{aligned}$$

$\gamma\gamma \rightarrow WW$ and $\gamma\gamma \rightarrow ZZ$: EFT interpretations

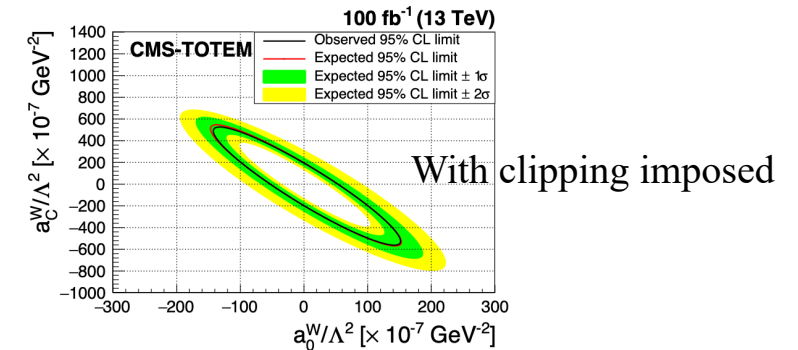
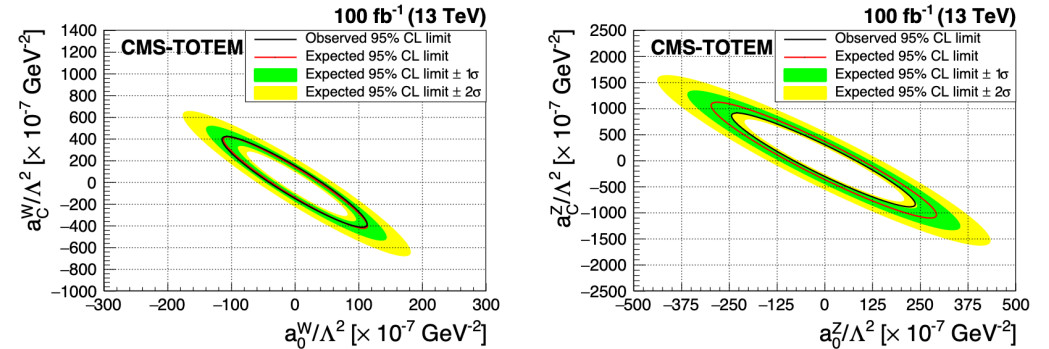
Event Reco and selection:

- The scattered protons are reconstructed using “Multi-RP Algorithm”. which combines tracks reconstructed in both tracking Roman pots in each arm of PPS.
- Both weak bosons decaying into boosted and merged jets.
- Proton jet matching is performed, and signal regions are defined using variables $1 - m(VV)/m(pp)$ and $y(pp) - y(VV)$.

Backgrounds:

- QCD multijet, $W + jets, Z + jets, t\bar{t}$. Have to rely on data for background estimate as the protons predominantly arise from diffractive pileup interactions, which are not well modelled.

Coupling	Observed (expected) 95% CL upper limit No clipping	Observed (expected) 95% CL upper limit Clipping at 1.4 TeV
$ a_0^W/\Lambda^2 $	$4.3 (3.9) \times 10^{-6} \text{ GeV}^{-2}$	$5.2 (5.1) \times 10^{-6} \text{ GeV}^{-2}$
$ a_C^W/\Lambda^2 $	$1.6 (1.4) \times 10^{-5} \text{ GeV}^{-2}$	$2.0 (2.0) \times 10^{-5} \text{ GeV}^{-2}$
$ a_0^Z/\Lambda^2 $	$0.9 (1.0) \times 10^{-5} \text{ GeV}^{-2}$	—
$ a_C^Z/\Lambda^2 $	$4.0 (4.5) \times 10^{-5} \text{ GeV}^{-2}$	—



Expected and observed limits on dimension-6 AQC operators